

From the Department of Experimental Surgery – Cancer Metastasis,

Medical Faculty Mannheim, University of Heidelberg

(Director: Prof. Dr. med. Heike Allgayer, MD, PhD)

Understanding the role of miR-122-5p in colorectal cancer liver metastasis

Inauguraldissertation

zur Erlangung des medizinischen Doktorgrades

der

Medizinischen Fakultät Mannheim

der Ruprecht-Karls-Universität

zu

Heidelberg

by

Sha Guan

From Hubei, the P. R. China

2017

Dekan: Prof. Dr. med. Sergij Goerdts

Referentin: Prof. Dr. med. Heike Allgayer, PhD

TABLE OF CONTENTS

ABBREVIATIONS	3
1 INTRODUCTION	4
2 AIM OF PROJECT	12
3 MATERIALS AND METHODS.....	13
3.1 Materials	13
3.1.1	13
3.1.2	13
3.1.3	13
3.1.4	16
3.1.5	16
3.1.6	16
3.2 Methods	17
3.2.1	17
3.2.2	17
3.2.3	18
3.2.4	18
3.2.5	19
3.2.6	19
3.2.7	19
3.2.8	21
3.2.9	21
3.2.10	22
3.2.11	23
3.2.12	24
3.2.13	24
3.2.14	25

3.2.15	25
3.2.16	26
3.2.17	26
3.2.18	27
3.2.19	27
3.2.20	28
3.2.21	28
 4 RESULTS	 29
4.1.....	29
4.2.....	30
4.3.....	32
4.4.....	32
4.5.....	34
4.6.....	35
4.7.....	36
4.8.....	37
4.9.....	38
4.10.....	39
4.11.....	43
 5 DISCUSSION.....	 45
 6 CONCLUSION.....	 45
 7 REFERENCE	 55
 8 CURRICULUM VITAE	 63
 9 ACKNOWLEDGEMENTS	 64

Abbreviations

ABL1	ABL proto-oncogene 1, non-receptor tyrosine kinase
B2M	Beta-2 microglobulin
CDKN1A/P21	Cyclin-dependent kinase inhibitor 1A
CRC	Colorectal Cancer
DTC	Disseminated Tumor Cell
FBS	Fetal Bovine Serum
GDP	Guanosine diphosphate
GIT1	G protein-coupled receptor kinase interacting ArfGAP 1
GRB7	Growth factor receptor-bound protein 7
GTP	Guanosine triphosphate
HCV	Hepatitis C virus
ITGAL	Integrin, alpha L
miRNA	microRNA
PBS	Phosphate Buffered Saline
PCR	Polymearase Chain Reaction
Pri-miRNA	Primary microRNA
Pre-miRNA	Preliminary microRNA
qPCR/RT-PCR	real-time quantitative polymerase chain reaction
RABL6/C9orf86	RAB, member RAS oncogene family-like 6
RIMS1	Regulating synaptic membrane exocytosis 1
RIPA	Radioimmunoprecipitation assay (buffer)
RNU6-2	U6 small nuclear 2 RNA
RRN18S	18S ribosomal RNA
SNO68	Small nucleolar RNA 68

1 INTRODUCTION

Colorectal Cancer (CRC) is the third most frequently diagnosed cancer and fourth leading cause of cancer death in males worldwide, and remains the second and third in females, respectively (Torre et al., 2015). The incidence and mortality have varied gradually over past decades. Some areas with historically low incidences like Western Asia and Eastern Europe are witnessing an increase, while the trend is declining in the United States, probably due to the increased use of screening (Siegel et al., 2017; Torre et al., 2015). However, there are still approximately 1.4 million cases and more than 0.6 million deaths every year (Jemal et al., 2011; Torre et al., 2015). Metastasis is the leading cause of CRC deaths and the liver is the most common metastasis site. Nearly 50% - 60% CRC patients are diagnosed with synchronous metastases, 80% of which have liver metastases (Stangl, Altendorf-Hofmann, Charnley, & Scheele, 1994; Yoo, Lopez-Soler, Longo, & Cha, 2006). Surgery is still advocated even in the absence of liver metastasis and 5-year survival rates are lower in patients with liver metastasis not undergoing surgery (Van Cutsem et al., 2006). Besides surgery, for disseminated CRC, there are systemic therapies including various drugs, either in combination or as single agents. Although these methods have prolonged patients' survival, outcomes are still far from desirable (Bosset et al., 2014). Tumor heterogeneity occurring throughout the progression and dissemination processes account for the low response rates of single drugs (Wolpin & Mayer, 2008). The process is made more complex by the various molecular regulators that are involved.

The Metastasis cascade

Metastasis is multistage process with an orderly sequence of basic steps comprising local invasion, intravasation, survival in the circulation, extravasation, formation of micrometastasis and colonization (Poste & Fidler, 1980; Steeg, 2006). These steps are often broken down into two main phases; that of the physical dissemination of tumor cells from the primary tumor to distant tissues, and that of the adaptation of these cells to foreign microenvironments resulting in successful colonization (McGowan, Kirstein, & Chambers, 2009; Peinado, Lavotshkin, & Lyden, 2011; Talmadge & Fidler, 2010). Considerably, evidence has recently surfaced indicating that cells can disseminate remarkably early, dispersing from seemingly noninvasive premalignant lesions in both mice and humans (Coghlin & Murray, 2010; Klein, 2009). Contrary to earlier assumptions, oncogenic transformation on its own is insufficient to confer metastatic competence, as demonstrated by

the observation of patients with disseminated tumor cells (DTCs) that do not develop overt clinical metastasis and that of many oncogene driven mouse models of cancer that failed to establish distant metastasis (Klein, 2003; Minna, Kurie, & Jacks, 2003). Furthermore, failure or insufficiency at any of the steps is a potential rate limiting step and could stop the entire cascade (Nguyen, Bos, & Massague, 2009).

Metastasis begins with a loss of cell-cell adhesion, which is the prerequisite for dissociation of tumor cells from the primary tumor. Thereafter, local invasion and migration into the surrounding tissue occurs via the proteolytic degradation of the extracellular matrix. After intravasation into the peripheral blood circulation, the cells must first escape the immune defenses, adhere to a vessel wall somewhere in the body, and finally invade into the tissue and establish a secondary tumor (Coghlin & Murray, 2010; Jiang, Puntis, & Hallett, 1994). Induction of neoangiogenesis ensures the growth of the metastasis and the sufficient supply of nutrients (Carmeliet & Jain, 2011).

The proteolytic degradation of extracellular matrix structures and basement membranes during metastasis is carried out by various tumor-associated protease systems, such as serine, aspartate, cysteine and threonine metalloproteinases (Blasi & Carmeliet, 2002; Geho, Bandle, Clair, & Liotta, 2005; Kessenbrock, Plaks, & Werb, 2010). These enzymes do not differ from those that control physiological processes such as wound healing, inflammation, embryogenesis or angiogenesis (Dvorak, 1986; Kessenbrock et al., 2010). Rather, the overexpression of these enzymes is the defining characteristic of the invasive phenotype of malignant cells.

Metastatic colonization

A prominent feature of metastasis is the ability of different tumor types to colonize the same or different organ sites, but interestingly, different tumor types tend to metastasize to specific organ sites with certain tumor types showing a limited range of target tissues. In the initial phases, most disseminated tumor cells are likely to be poorly adapted to the microenvironment of the tissue in which they have settled. An acclimatization to this new environment needs to occur requiring colonization programs that are often tumor specific and dependent on the nature of the ‘would be’ colonized tissue microenvironment. Organ specific colonization functions in the case of bone metastasis are relatively well established, and for example, the ability of breast cancer cells to form typical osteolytic metastasis requires the

production of osteoclast activating factors PTHRP, IL-11, IL-6, TNF α and GM-CSF. GM-CSF directly promotes osteoclastogenesis while the rest of the cytokines induce osteoclast formation via the induction of RANKL, a nuclear factor- κ B ligand. The expression of these secreted factors would be unlikely to provide a selective advantage in another metastatic site or in the primary tumor but are essential to the development of osteolytic lesions. The mediators of colonization in other organ microenvironments such as the brain and liver remain unknown (Nguyen et al., 2009).

The liver is a common metastasis site for several solid tumors, especially that of the gastrointestinal tract. In addition, the liver is also colonized by hematogenous tumors such as myelomas and leukemias. Its unique biology and anatomical location renders the liver particularly receptive to circulating disseminated tumor cells. The two sources of its unique dual blood supply (80 percent deoxygenated blood via the portal vein and 20 percent oxygen-rich blood via the hepatic artery) come together at the point of entry into the sinusoids, and the mixed blood supplies the liver parenchymal cells before draining via the centrilobular veins. Circulating tumor cells can enter the liver through both vascular entry ports.

The normal liver actually displays inherent architectural and functional features which favor metastasis. These features include: (a) a liver-specific microcirculation with its unique sinusoidal cell population, (b) perivascular mesenchymal cells including hepatic stellate cells (HSCs), (c) a morphologically and metabolically heterogeneous parenchymal cell compartment, and (d) the hepatic regional immunity (Kruger, 2015). The distinctive circulatory network in the hepatic sinusoids positively contributes to the retention of disseminated tumor cells in the liver (**Figure 1**).

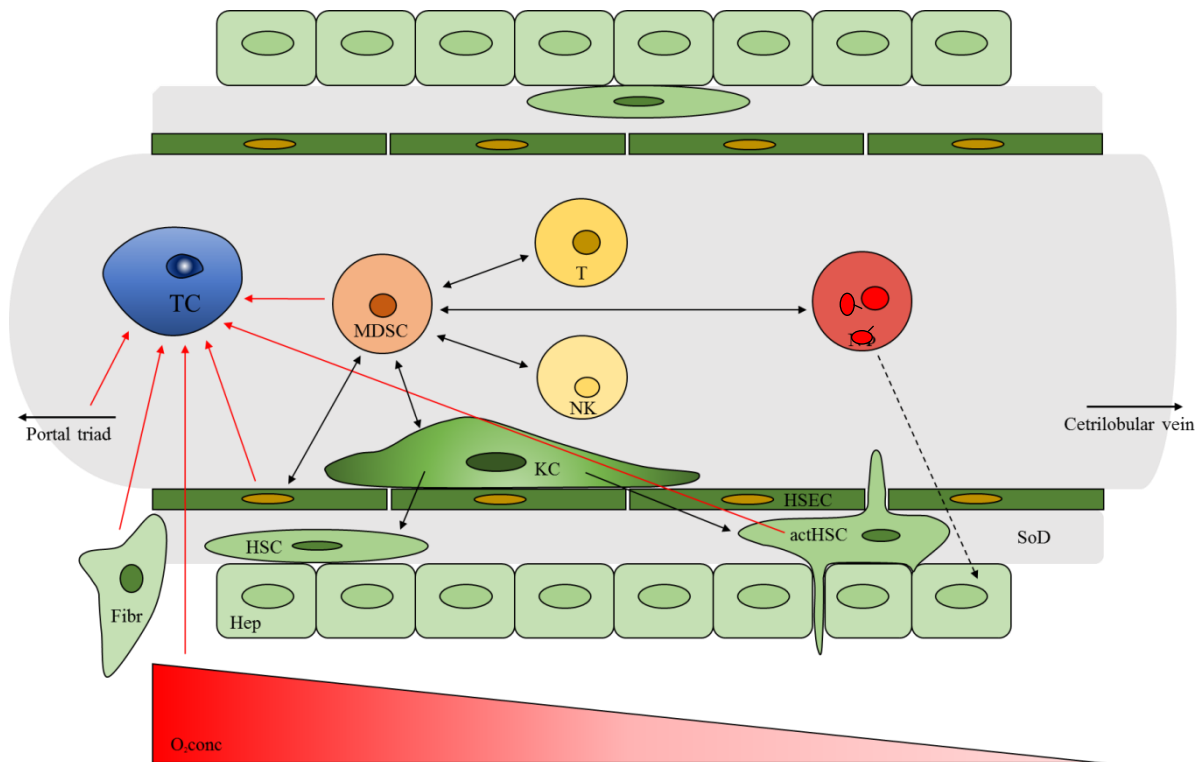


Figure 1. Inherent features of hepatic sinusoids favor metastasis (red arrows): Connection of sinusoids and primary tumour sites via the blood circulation and entry of TCs via the portal triad; perivascular portal tract fibroblasts and HSCs secrete prometastatic factors; slow blood flowing in microcirculation promoting attachment of TCs to HSECs; metabolically heterogeneous parenchymal cells and oxygen gradient; regional immune suppression by interactions of MDSCs with other immune cells and activated HSC (black arrows). Invasion of mature neutrophils (Dotted arrow). Fibr portal tract fibroblasts, Hep hepatocyte, HSC hepatic stellate cells, actHSC activated hepatic stellate cells, KC Kupffer cells, MDSC myeloid-derived suppressor cells, NK natural killer cells, NΦ neutrophil granulocytes, O₂conc oxygen concentration, SoD space of Disse, TC tumour cell, T T lymphocyte. Figure adapted from (Kruger, 2015).

Four major phases have been described in the progression of liver metastasis: (1) the microvascular phase, including tumor cells arrest in the sinusoidal vessels, can lead to tumor cell death or extravasation; (2) the extravascular, pre-angiogenic phase, during which avascular micrometastases appear via recruitment of host stromal cells ; (3) the angiogenic phase, during which endothelial cells are initiated and the tumors become vascularized via interactions with the microenvironment; and (4) the growth phase, which leads to the establishment of ‘clinical’ metastases (Van den Eynden et al., 2013).

MicroRNAs

MicroRNAs (miRNAs) are small non-coding RNA molecules (18-22 nucleotides) that regulate gene expression (Ambros, 2004). The human genome encodes over 1000 miRNAs (Bentwich et al., 2005), which appear to target about 60% of the protein coding genes (Lewis, Burge, & Bartel, 2005). miRNA genes are usually transcribed by RNA polymerase II. The resulting transcript is a spliced stem-loop precursor with a 5' cap and a poly (A) tail called primary miRNA (pri-miRNA) (Lee et al., 2004). A single pri-miRNA may contain one to six miRNA precursors. A pri-miRNA is cut by the DiGeorge Syndrome Critical Region 8 (DGCR8), and Drosha enzymes, resulting in the formation of a precursor-miRNA (pre-miRNA) (Conrad, Marsico, Gehre, & Orom, 2014). These are then exported out of the nucleus and cut by the RNase enzyme, Dicer. The final product is a mature miRNA about 18~22 nucleotides in length (Lund & Dahlberg, 2006) (**Figure 2**).

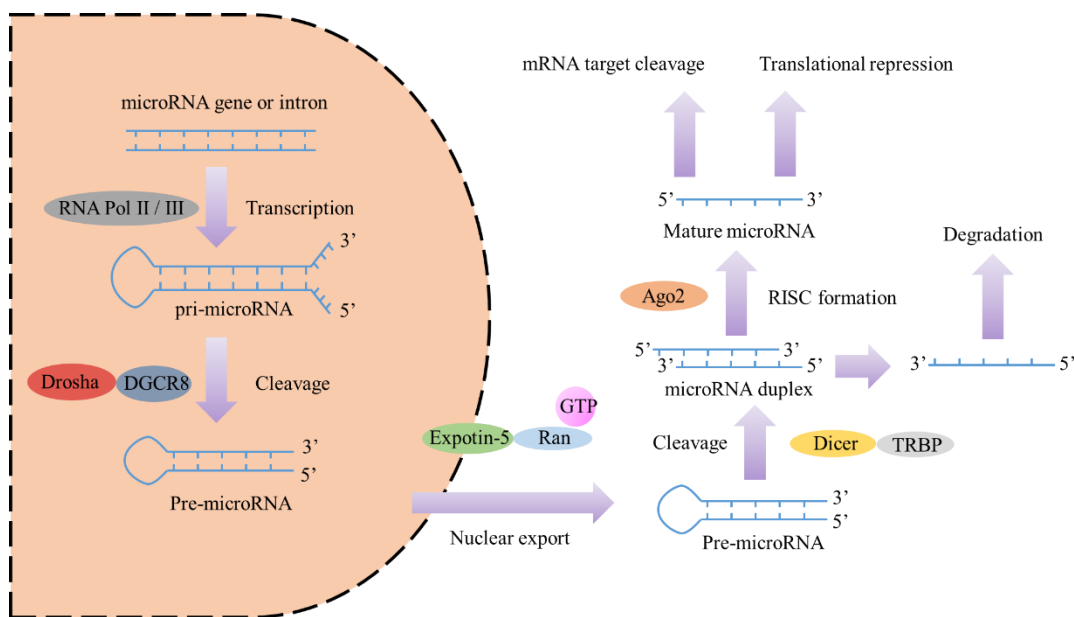


Figure 2. Schema of microRNA biogenesis. Figure adapted from (Winter, Jung, Keller, Gregory, & Diederichs, 2009).

miRNAs function in cell regulation. A miRNA is complementary to a part of one or more messenger RNAs (mRNAs). Animal miRNAs are usually complementary to the 3' UTR (X. J. Wang, Reyes, Chua, & Gaasterland, 2004) in a manner that is usually imperfect. miRNAs normally inhibit the protein translation of target mRNAs (Williams, 2008) but some miRNAs augment the degradation of mRNAs (Eulalio et al., 2009).

Most miRNAs are located within cells but some of them can be found in the extracellular environment like culture media and function in cell-cell signaling (Turchinovich, Weiz, & Burwinkel, 2012).

MicroRNAs in Cancer and Cancer Metastasis

Several miRNAs have been linked to cancer. MicroRNAs are deregulated in an array of solid cancers, as well as hematological malignancies (Lu et al., 2005). The finding that miRNAs have a role in cancer is reinforced by the fact that about 50 percent of miRNA genes are located in cancer associated genomic regions, or in fragile sites. The list of cancer-associated miRNAs is growing very rapidly. The deregulation of certain miRNAs has been shown to cut across several cancer types, for instance miR-21 is commonly up-regulated in breast, colon, lung, pancreas, prostate, stomach, cervical, ovarian, hepatobiliary and head and neck cancers as well as in B-cell lymphoma and chronic lymphocytic leukemia (Lu et al., 2005; Volinia et al., 2006).

A significant number of miRNAs have been identified to be linked with CRC, such as miR-10b (Baffa et al., 2009), miR-451 (Bitarte et al., 2011), miR-135b (Gaedcke et al., 2012), miR-224 (Ling et al., 2016), et al. In some of the published reports, the affected target proteins and implicated pathways identified were linked to the prediction and prognosis of metastasis in CRC. Since metastasis is the main cause of mortality, a lot of research has been focused on the difference between primary cancer and metastases like liver metastases. For instance, let-7i and miR-10b were significantly downregulated in liver metastases compared with primary CRC (Hur et al., 2015).

The Allgayer group has done a considerable amount of work on miRNAs and colorectal cancer metastases (Asangani et al., 2008; Ceppi et al., 2010; Kumarswamy et al., 2012; Laudato et al., 2017; Mudduluru et al., 2011). The group identified an exclusive miRNA signature that is differently expressed in metastases. Three of these miRNAs were identified as key drivers of an EMT-regulating network acting through a number of novel targets including SIAH1, SETD2, ZEB2 and especially FOXN3, which suppress the transcription of N-cadherin. The modulation of N-cadherin impacted on the migration, invasion and metastasis of cancer cells (Mudduluru et al., 2015). Similarly, the group found the miRs-134 and -370 to be potential tumor suppressor miRNAs that could suppress colorectal cancer tumorigenesis by regulating the EGFR signaling cascade (El-Daly, Abba, Patil, & Allgayer,

2016).

miR-122

miR-122 is highly abundant and specific to the liver and this microRNA plays a critical role in liver homeostasis by regulating the expression of a large number of target mRNAs and also by suppressing non-hepatic genes (Fu et al., 2005; Landgraf et al., 2007). It is normally known to be involved in the regulation of numerous transcripts encoding a variety of hepatic processes, like cholesterol and lipid metabolism (Esau et al., 2006), mitochondrial function (Burchard et al., 2010), polyploidy regulation (Hsu et al., 2016), hepatitis C virus replication (Jopling, Yi, Lancaster, Lemon, & Sarnow, 2005), and liver tumor suppression (Tsai et al., 2009). Hepatic and circulating levels of miR-122 are a prognostic marker in patients with hepatocellular carcinoma (Coulouarn, Factor, Andersen, Durkin, & Thorgeirsson, 2009).

Several liver-enriched transcription factors, e.g. C/EBP α , HNF1 α , HNF3 β , and HNF4 α (Coulouarn et al., 2009; Xu et al., 2010) and HNF6 (Laudadio et al., 2012) were shown to activate miR-122 gene expression in hepatic cell lines. Furthermore, miR-122 has been identified to regulate a large set of target genes. In fact, the first miR-122 target identified was the gene cationic amino acid transporter 1 (CAT-1) or Slc7a1 (J. Chang et al., 2004), which is expressed in many other adult tissue types and strongly expressed in fetal liver, yet under normal un-stressed circumstances, is repressed in adult hepatocytes (Krutzfeldt et al., 2005). As a tumor suppressor, miR-122 suppresses c-Myc transcription by targeting E2f1, a transcriptional activator, and Tfdp2, a co-activator. Whereas c-Myc suppresses miR-122 expression directly by binding to its promoter region and indirectly by downregulating several liver enriched transcription factors (B. Wang et al., 2014). There are other oncogenes identified as its targets, such as cyclin G1, involved in G2/M arrest in response to DNA damage (S. Wang et al., 2012), RhoA, a member of the Rho family of small GTPases associated with tumor cell proliferation and metastasis (S. C. Wang et al., 2014), and BCL-w, an anti-apoptotic Bcl-2 family member (Lin, Gong, Tseng, Wang, & Wu, 2008). However, despite a lot of existing data on miR-122 and its association with tumorigenesis (**Figure 3**), a complete description of the miR-122-regulated target network, especially in metastasis remains incomplete.

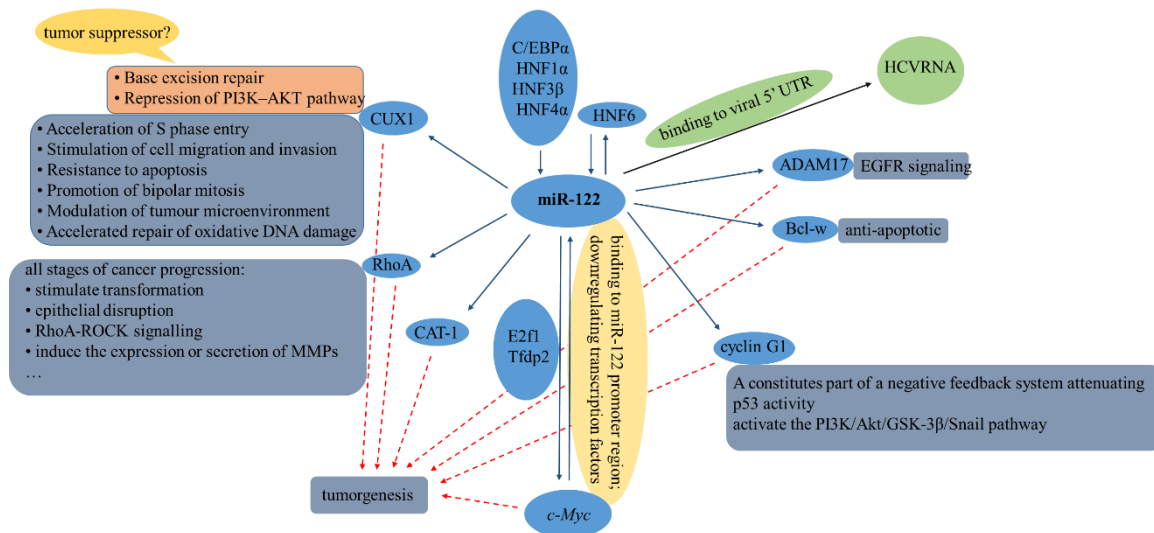


Figure 3. The network of parts of the interactions between miR-122 and its main identified target genes (blue circles) for the regulation of HCV (Hepatitis C virus) replication (green circles) and tumor related processes (normally focus on hepatocellular carcinoma) (red and grey circles) (J. Chang et al., 2004; Hsu et al., 2016; Lin et al., 2008; Tsai et al., 2009; B. Wang et al., 2014; S. Wang et al., 2012; S. C. Wang et al., 2014).

As a prelude to this project, the whole genomes of 12 patients with advanced colorectal cancer were sequenced with the Illumina next generation sequencing platform at the Allgayer department. Bioinformatics analysis and subsequent validation showed that the miR-122 gene locus was deleted in primary tumors and corresponding metastases of most patients. Interestingly, while the expression of miR-122 was suppressed in primary tumors, it was significantly increased in metastatic lesions. This, however, contrasted to the additional observation at the genome level.

2 AIM OF THE PROJECT

The aim of this project was to investigate the role of miR-122 in colorectal cancer liver metastasis. The specific objectives were to:

- 1) Identify putative targets of miR-122 that could play a role in metastasis
- 2) Validate the identified targets with 3'UTR reporter gene assays and evaluate the specificity of the miRNA/target interactions
- 3) Evaluate the impact of miR-122 on the expression of the identified targets
- 4) Investigate the mechanisms of miR-122 activity in the context of liver metastasis
- 5) Identify metastasis related functions impacted by miR-122

3 MATERIALS AND METHODS

3.1 Materials

3.1.1 Cell lines

The RKO, CaCo2, SW48, SW480, SW620, HCT116, HT1080, DLD-1, Colo-320 (human colorectal), and 239T (mouse embryonic kidney) cell lines were obtained from the American Type Culture Collection (ATCC). The Huh7 and Hep3B cell lines were kind gifts from Drs. Rodriguez-Vita and Clemm von Hohenberg both of the German Cancer Research Center (DKFZ), respectively. The cell lines were maintained in the recommended media supplemented with 10% FBS. All cells were cultured in a humidified incubator at 37 °C with 5% CO₂.

3.1.2 Plasmids

Empty vector plasmid pLightSwitch 3' UTR plasmid was purchased from SwitchGear Genomics (Menlo Park, USA).

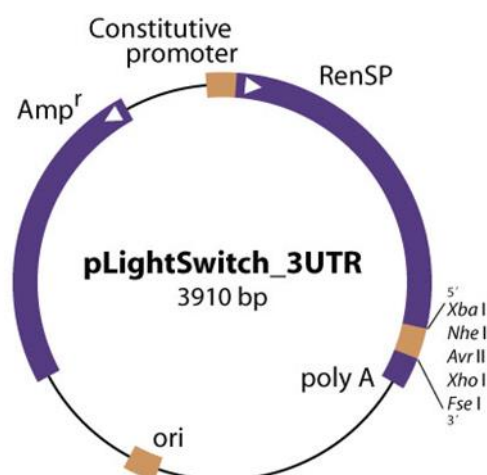


Figure 4. pLightSwitch 3' UTR plasmid structure

<http://switchgeargenomics.com/resources/vector-maps/3utr-reporter-vector>

3.1.3 Primers

3'UTR cloning primers

Gene name	Gene symbol	Forward primer (Tm [°C])	Reverse primer (Tm [°C])
Regulating	synaptic <i>RIMS1</i>	AATATGCTAGCTGAACTCATAC	CCGCGCTCGAGGACATGAA AAGTAAATTTTATTAAA

membrane exocytosis 1		CAGAGTCATTCCAA (72.1)	(70.9)
RAB, member RAS oncogene family-like 6	<i>RABL6/C9orf86</i>	ATTAATGCTAGCGCCGGCGTGG GCAGTGGCCGCCCTG (84.6)	GCCGGCCTCGAGCAGAGTG AAACAGGAGTGCTTTATG (80.1)
ABL proto-oncogene 1, non-receptor tyrosine kinase	<i>ABL1</i>	TTAATTAGCTAGCCAGCAGTCA GGGGTCAGGTGTCAGG (79.1)	CCGGCCGCTCGAGCTAATG TAAACACTGATTTATTAA (74.5)
G protein-coupled receptor kinase interacting ArfGAP 1	<i>GIT1</i>	AATTAGCTAGCCCTCTCTCCCC ACACCCTCACCTGC (79.9)	GGCCGCTCGAGAACAGCTC ATGGTCACTTCTTTATT (76.6)
Growth factor receptor- bound protein 7	<i>GRB7</i>	TTAAATTAGCTAGCCCAGGCCG TGGACTGGCTCATGCCT (80.0)	GGCCCGGCCTCGAGGTATC AAAAAATAATCTTTATTGT C (75.9)
Integrin, alpha L	<i>ITGAL</i>	AATTAGCTAGCGTCCAGGCCTG TGAGGTGCAGAGTG (79.1)	GGCCGCTCGAGGGACAGA ATTTCACATTTATTGGAT (75.4)

Site-directed mutagenesis primers:

Gene symbol	Forward primer (Tm [°C])	Reverse primer (Tm [°C])
<i>RIMS1</i>	1 cagaaatgtgtagaatacaacttttcacatctgtagagttcc agttgttcaattgggtgtgtgtgt (78.19)	acacacacacacaaattgaacaaactggaaactctacag atgtgaaaagttgtattctacacatttctg(78.19)
	2 Cattttttaatatcaggaagaaaaaggcattacaagtctgtt tttcaagtacaattatgcagttagtttagtcccca (78.09)	Tggggactaaaactaactgcataattgtactttgaaaaaca gacttgtaatgcctttttctctgatattaaaaaatg (78.09)
	3 Atgctgctctatttgtgaatcacaaaagtgtctgtactcata aaaggaggagagaacatatcaatgc (78.04)	Gcattgatatgttctccctcctttatgagtacagacactttt gtgattacacaaatagagcagcat (78.04)
	4 Attggaatttcatttaaaagcacagggtctgtttaagacaag tggtcaaaatagaagatactaccaattataatcag (78.56)	Ctgattataattgggtagtatctttctatttggaccactgtctt aaacagaccctgtgcttttaaatgaaattccaat (78.56)

<i>RABL6/ C9orf86</i>	1	Ctgagtggagtgtttgggagtctgtcctcccggtcctgcc ttcg (79.08)	Cgaaggcaggagccgggaggacagactcccaaacact ccactcag (79.08)
	2	Ggagtgctttatggctgagtgtctgttttgggagtctgtcct cccggt (78.50)	Agccgggaggacagactcccaaacagacactcagac cataaagcactcc (78.50)
<i>GIT1</i>	1	Tggggtggggattaatgtctgtctgtgccagctcctatgg ccagt (78.31)	Cactggccataggagctgggcacagacagacattaatcc ccaccca (78.31)
	2	Acctggctgccaggtctgttggcagcactaagggcacttg tgcca (78.17)	Tggcacaagtgcccttagtctgccaacagacctggcag ccaggt (78.17)
	3	Aggcgaggggctggtctgtatgccttcagggccctgtc act (78.97)	Agtgagcaggggcctgcaaggcatacagaccagccct cgcct (78.97)
	4	Cggagagctgccccactgtctgttccccacctgcccttt gc (78.97)	Gcaaaggggcaggtggggaacagacaagtggggcag ctctccg (78.97)
	5	Aagttcatagagaaggggcatctgtgggaggatcagg gaggcagc (78.31)	Gctgcctccctgatccctccacagatcgecccttctctat gaactt (78.31)
<i>GRB7</i>	1	Caaagaagcagaggagaaaactgtctgtcggaaccctc ccgtctctcatc (79.36)	Gatgaggagcgggagggtccgcacagacagttttctcc tctgttctttg (79.36)
	2	Gagaggggtcaggagtggactgtctgtgggctgtttct atctgaggg (79.28)	Ccctcagatagaaaacagccccacagacagtccactcct gacctctc (79.28)
	3	Ttcccttgaggagaggggtcagtctgtgactgtctgtggg gctgtttc (78.44)	Gaaaacagccccacagacagtcacagactgacctct cctcaaggga (78.44)

RT-PCR primers

RT-PCR primers were purchased from QIAGEN; RIMS1 (Cat# QT01016673), RABL6 (Cat# QT00105042), and for internal control B2M (Cat# PAHS-000Z), RRN18S (Cat# QT00199367). The primers for miRNAs were also purchased from QIAGEN; miR-122 (Cat# MS00003416) and for internal control RNU6-2_11 (Cat# MS00033740).

3.1.4 miRNA mimics and inhibitors

miR-122 mimic and inhibitor were purchased from from Ambion, Life Technologies (miR-122 mimic ID: MC11012 and inhibitor ID: MH11012).

3.1.5 Antibodies

Primary antibodies

Antibody anti-	Species/isotype	Dilution for WB	Supplier
RIMS1 IgG	Rabbit	1:5000	Alomone labs
RABL6 IgG	Rabbit	1:5000	ThermoFisher
β -actin IgG	Rabbit	1:10000	Abcam

Secondary antibodies

Antibody anti-	Dilution for WB	Supplier
Rabbit IgG	1:10000	Cell Signaling
Mouse IgG	1:10000	Cell Signaling

3.1.6 Kits

Products	Supplier
QIAamp [®] DNA Mini kit	QIAGEN
miScript II RT Kit	QIAGEN

Qiaquick® Gel Extraction Kit	QIAGEN
Qiaquick® PCR Purification Kit	QIAGEN
QIAprep® Spin Miniprep Kit	QIAGEN
miRNeasy® Mini Kit	QIAGEN
exoEasy Maxi Kit	QIAGEN
exoRNeasy Serum/Plasma Starter Kit	QIAGEN
CellTiter 96® Aqueous One Solution Cell Proliferation Assay	Promega

3.2 Methods

3.2.1 Cell culture

Cells were cultured routinely in T25 flasks at 37°C in the presence of 5% CO₂ and 90% humidity. Culture media were cell line specific (Gibco GmbH, Germany) and supplemented with 10% FBS (Sigma-Aldrich). Depending on growth rate, cells were passaged as necessary. The routine procedure consisted of washing the cells with PBS (Gibco GmbH, Germany) and adding trypsin (Gibco GmbH, Germany) to cover the cells, followed by a 3-5 min short incubation at 37°C to aid detachment. The cells were then observed under a microscope to confirm detachment. A minimum of 3 volumes in excess of trypsin, of complete medium (with FBS) was added to the cells, pipetted up and down several times to ensure a single cell suspension, centrifuged to remove excess trypsin, re-suspended in medium and distributed into new flasks in the required dilution and topped up with medium requisite of the flask.

3.2.2 Co-culture

Huh7 cells were plated in the bottom of 12mm Transwell® with 0.4µm Pore Polyester Membrane Insert (Costar) 2 days before RKO cells. Each well contains 200,000 Huh7 cells initially. RKO cells were plated into the top small well 2 days later for 100,000 cells per well.

After 48 or 72 hours, total RNA of RKO cells in the top well was collected by miRNeasy® Mini Kit (QIAGEN).

3.2.3 Transfection

Two different colorectal cancer cell lines (HCT116 and RKO) were used for transfection with miRNA-mimics, -inhibitors, and their corresponding scrambled controls. Mimics and inhibitors were transfected at a final concentration of 150 nM using the METAFECTENE® (Biontex Laboratories GmbH). The cells were incubated for 24–72 hours following transfection before proceeding with experiments.

3.2.4 RNA Isolation

Total RNA including miRNA was extracted and purified from cell lines using Qiagen's miRNeasy Mini Kit according to the manufacturer's protocols. The cells were disrupted by adding 700 µl QIAzol Lysis Reagent (QIAGEN) and pipetting to mix. The lysate was transferred into a microcentrifuge tube. Then the tube was placed on the benchtop at room temperature (15–25°C) for 5 min. 140 µl chloroform was added into the tube and shake the tube vigorously for 15 s. Place the tube on the benchtop at room temperature for 2–3 min. Centrifuge for 15 min at 12,000 x g at 4°C. After centrifuge, the upper aqueous phase in the tube was transferred to a new collection tube. 1.5 volumes (usually 525 µl) of 100% ethanol was added and mix thoroughly by pipetting up and down several times. The sample was added into an RNeasy Mini spin column in a 2 ml collection tube (supplied in the kit) and was centrifuged at $\geq 8000 \times g$ ($\geq 10,000$ rpm) for 15 s at room temperature (15–25°C). The flow-through was discarded. 700 µl Buffer RWT was added to the RNeasy Mini spin column and centrifuged for 15 s at $\geq 8000 \times g$ ($\geq 10,000$ rpm) to wash the column. 500 µl Buffer RPE was added onto the RNeasy Mini spin column and centrifuged for 15 s at $\geq 8000 \times g$ ($\geq 10,000$ rpm). Another 500 µl Buffer RPE was added to the RNeasy Mini spin column and centrifuged for 2 min at $\geq 8000 \times g$ ($\geq 10,000$ rpm) to dry the RNeasy Mini spin column membrane. In the end, 30–50 µl RNase-free water was added directly onto the RNeasy Mini spin column membrane and centrifuge for 1 min at $\geq 8000 \times g$ ($\geq 10,000$ rpm) to elute the RNA. RNA can be stored at -80°C. The concentration of RNA was measured by NanoDrop™ 2000 Spectrophotometer (ThermoFisher).

3.2.5 DNA Isolation

Genomic DNA was extracted with the QIAamp[®] DNA Mini kit from 293T cell line according to the given protocol. In summary, cell pellets were re-suspended in 200 µl PBS and 200 µl Buffer AL was added to the sample. Mix by pulse-vortexing for 15 s. The mixture was incubated at 56°C for 10 min. 200 µl ethanol (96–100%) was added to the sample, and pulse-vortexed for 15 s. After mixing, the mixture was applied to the QIAamp Spin Column and centrifuged at 6000 x g (8000 rpm) for 1 min. 500 µl Buffer AW1 was added then and centrifuged at 6000 x g (8000 rpm) for 1 min. 500 µl Buffer AW2 was added and centrifuged at full speed (20,000 x g; 14,000 rpm) for 3 min. 200 µl Buffer AE or distilled water was added. Incubate at room temperature (15–25°C) for 1 min, and then centrifuge at 6000 x g (8000 rpm) for 1 min. The products can be stored at -20°C. The concentration of DNA was measured by NanoDrop[™] 2000 Spectrophotometer (ThermoFisher).

3.2.6 Reverse Transcription (cDNA synthesis)

Reverse transcription was performed to obtain the cDNA from RNA. Cell line RNA samples were thawed on ice. We used miScript II RT Kit (QIAGEN) and chose 5 × miScript HiFlex Buffer for the reverse transcription. Assemble the following reaction in a sterile microcentrifuge tube and incubate at 37°C for 1 hour and 95°C for 5 min. After reverse transcription, cDNA was diluted 10× and stored at -20°C.

Sample RNA	500ng
5 × miScript HiFlex Buffer	2µl
10 × miScript Reverse Transcriptase Mix	1u
10 × miScript Nucleics Mix	1µl
<u>Rnase-Free Water</u>	<u>Variable</u>
Final volume	10µl

3.2.7 PCR for amplification of 3'UTR

PCR setup for DNA from 293T cell line:

Term	End Concentration	Volume
10 × Qiagen PCR buffer	1 ×	1 µL
Forward Primer	0.2 µM	0.2 µL
Reverse Primer	0.2 µM	0.2 µL
dNTPs	0.2 mM	0.2 µL
Qiagen <i>Tag</i> DNA polymerase	0.5 unit/µL	0.1 µL
Water		Variable
DNA template (100ng)		Variable
Total volume of reaction		10 µL

PCR setup for 3'UTR cloning of *MIR122* targets

Gene	Initial Denat.	Denat.	Annealing	Extension	Final Extension	Cycles
<i>RIMS1</i>			58°C 45 sec	72°C 2 min		
<i>RABL6/C9orf86</i>			55°C 45 sec	72°C 1 min		
<i>ABL1</i>	94°C	94°C	55°C 45 sec	72°C 90 sec	72°C	35
<i>GIT1</i>	3 min	1 min	60°C 45 sec	72°C 30 sec	10 min	
<i>GRB7</i>			51°C 45 sec	72°C 2 min		
<i>ITGAL</i>			62°C 45 sec	72°C 2 min		

3.2.8 Realtime-PCR

Realtime-PCR was used to quantify miR-122 expression in different cell lines or cells under different interfering. Real-time PCR was performed using Fast SYBR™ Green Master Mix (Applied Biosystems™). All samples were normalized to the internal control (B2M or RNU6) and fold changes were calculated with the $2^{-\Delta\Delta C_t}$ method.

Term	End Concentration	<i>MIR122</i>	<i>RNU6</i>
Fast SYBR™ Green Master Mix	1 ×	5 μL	5 μL
10 × Primers	1 ×	1 μL	1 μL
Universal primer	0.5 μM	1 μL	1 μL
Water		1 μL	1 μL
cDNA template (1:10 diluted)		2 μL	2 μL
Total volume of reaction		10 μL	10 μL

Term	Final Concentration	<i>RIMS1</i>	<i>RABL6</i>	<i>B2M</i>
Fast SYBR™ Green Master Mix	1 ×	5 μL	5 μL	5 μL
10 × Primers	1 ×	1 μL	1 μL	1 μL
Water		2 μL	2 μL	2 μL
cDNA template (1:10 diluted)		2 μL	2 μL	2 μL
Total volume of reaction		10 μL	10 μL	10 μL

3.2.9 Colony PCR

Single colonies were picked and suspended in 100 μl Milli-Q water. Meanwhile a regular PCR with pLightSwitch_3UTR plasmid primers (Forward: GGGAAGTACATCAAGAGCTTCGT; Reverse: CCCCCTGAACCTGAAACATAAA) and gel analysis were performed to verify the

insert DNAs. The correct ones were added into 5ml LB medium with Ampicillin respectively and shaken overnight at 37°C. QIAprep® Spin Miniprep Kit was used to extract and purify plasmids from *E.coli* (One Shot™ TOP10 Chemically Competent *E. coli*, Invitrogen™). Two to 3 clones of each 3'UTR were sequenced to identify correctly cloned 3'UTRs.

3.2.10 Plasmids

The restriction sequences for the chosen restriction enzymes were already incorporated to the forward and reverse primers of the target genes of miR-122. The restriction digest reaction (Nhe I 10,000 u/ml and Xho I 20,000 u/ml, New England BioLabs) were assembled in a sterile microcentrifuge tube and incubated at 37°C for 1 hour. For the pLightSwitch, plasmid vector, 1ul of Shrimp Alkaline Phosphatase (SAP, 1 u/μl) (Fermentas) was added for 1 hour at 37°C after the digestion. The DNA products were purified with the Qiaquick® PCR Purification Kit according to the protocol as described in **3.2.14**.

DNA fragment or plasmid	1000 ng
Nhe I	1 μl
Xho I	1 μl
Cutsmart buffer	5 μl
Nuclease-Free Water to final volume of	50 μl

T4 DNA Ligase (5u/μl) (Fermentas) catalyzed the ligation of the amplified 3'UTR fragments to the pLightSwitch_3'UTR plasmid after the digestion with NheI and XhoI I. A 3:1 molar ratio of vector: insert DNA was used as following:

$$\frac{100\text{ng vector} \times \text{kb size of insert}}{3.9 \text{ kb vector}} \times \frac{3}{1} = \text{ng of insert}$$

Assemble the following reaction in a sterile microcentrifuge tube and incubate at room temperature overnight.

Vector DNA	100ng
Insert DNA	Variable

Ligase 10X Buffer 1µl

T4 DNA Ligase 1u

Nuclease-Free Water to final volume of 10µl

One Shot® TOP10 Chemically Competent E. coli (Invitrogen) were thawed on ice for half an hour. 10µl ligation reaction product was added into 50µl of competent cells and incubated on ice for 30 min. Then the cells were heat shocked for 45 sec at 42°C and immediately placed on ice for 5 min. 500µl LB (Luria Broth) medium was added into each tube and incubated for 1 hour at 37°C with vigorous shaking. The suspension was then applied on a LB agar plate containing Ampicillin. The plates were incubated overnight at 37°C. Single colonies were picked and then processed as in step **3.2.9**.

3.2.11 Site directed mutagenesis

PCR set up for site directed mutagenesis

10× reaction buffer 5 µl

dsDNA template (plasmids in **2.2.9** verified by sequencing) 50 ng

Oligonucleotide primer #1 250 ng

Oligonucleotide primer #2 250 ng

dNTP mix 1 µl

ddH₂O to a final volume of 50 µl

1 µl of Pfu DNA Polymerase (native) (2.5 u/µl) (Fermentas) was added to sample reaction. The cycling parameters outlined in the following table

Segment	Cycles	Temperature	Time
1	1	95°C	30 seconds
2	12	95°C	30 seconds

	55°C	1 minute
	68°C	2 minutes/kb of plasmid length

1 µl of the Dpn I restriction enzyme (10 u/µl) (BioLabs) was added after the cycles. Gently and thoroughly mix each reaction, spin down in a microcentrifuge for 1 minute, and immediately incubate at 37°C for 1 hour to digest the parental supercoiled dsDNA. 1 µl of the Dpn I-treated DNA was transfected into One Shot® TOP10 Chemically Competent E. coli as described previously in **3.2.10** and verified by sequencing.

3.2.12 Agarose gel electrophoresis

To validate the specificity of PCR products, gel analysis was performed. A 2% gel (3 g agarose powder dissolved in 150 mL 1 × TAE buffer) was used. For each sample analyzed, 10 µL PCR product, 5 µL 2 × loading dye and 1.5 µL 10 × Midori Green (NIPPON Genetics EUROPE GmbH) were loaded into the gel. 5 µL DNA ladder (100bp) was then loaded alongside the samples. The gel was run at 110 V for 1 h. The presence of only 1 band in each lane supported the specificity of the reaction.

3.2.13 Gel purification

The QIAquick Gel extraction kit (QIAGEN) was used for this application. Gel slices containing the desired fragment were cut with a scalpel under UV light, transferred to an eppendorf tube and weighed. The gel was dissolved by heating the slice in 3 equivalent volumes (gel) of QG buffer for 10 minutes (or longer if dissolution was not achieved) at 50°C.

One volume of the gel mass of isopropanol was added to the mixture, mixed properly, transferred into a QIAquick column and centrifuged for 1 min at 13000 rpm. The flow-through was discarded and 500 µl of buffer QG was added to the column and centrifuged for 1 min at 13000 rpm to remove the remaining traces of gel from the sample. Subsequently, 750 µl buffer PE was used to wash the column, which was centrifuged for an additional 1 min to remove the traces of the buffer. In between the steps the flow-through was discarded. The column was transferred into a fresh 1.5 ml eppendorf and the DNA eluted in 30 µl of elution buffer (EB). The eluate was quantified using the Nanodrop spectrophotometer and used directly or stored at -20°C until required.

3.2.14 Purification of PCR products

The QIAquick® PCR Purification Kit (QIAGEN) was used for this application. 5 volumes of Buffer PB were added to 1 volume of the PCR sample and mixed. The sample was applied to the QIAquick column and centrifuged for 30–60s. The flow-through was discarded. 0.75 ml Buffer PE was added to the QIAquick column and centrifuged for 30–60s. The flow-through was discarded and the QIAquick column placed back in the same tube. The column was centrifuged for an additional 1 min. Place QIAquick column. To elute DNA, 30 µl Buffer EB (10 mM Tris·Cl, pH 8.5) or water (pH 7.0–8.5) was added to the center of the QIAquick membrane placed in a clean 1.5 ml microcentrifuge tube, let to stand for 1 min, and then centrifuged for 1 min. The products were stored at -20°C. The concentration of DNA was measured with NanoDrop™ 2000 Spectrophotometer (ThermoFisher).

3.2.15 Western Blot

Cells were washed by PBS and added ice-cold RIPA buffer (200µl per well). Plates were kept on ice for 15 min. The cells were scraped into microfuge tubes and then spun at 12,000×g for 20 min at 4°C. The supernatant was transferred to fresh tubes and a small volume removed (10µl) to perform a BCA protein assay. 30-60µg of each sample was mixed with a quarter volume of 4× Laemmli sample buffer. Protein lysates were boiled at 95°C for 5 min and then centrifuged for 1 min.

Western Blot was used for the detection of RIMS1 and RABL6 proteins. The samples were loaded into 10% SDS-PAGE gels. The gel was run for about one and half hour at 100 V. The transfer sandwich was assembled avoiding bubbles. The PVDF blot was on the cathode and the gel on the anode. The cassettes were placed in the transfer tank and the tank placed in an icebox. Since RIMS1 protein is bigger than 150KD, the transfer was run for 150-180 min at 100 V. The blots were stained with Ponceau S solution to check the transfer quality and then washed with TBST. The blots were then blocked in 5% non-fat milk at room temperature for 1 hour followed by overnight incubation in a primary antibody solution at 4°C. The blots were rinsed 3 times with TBST and incubated in the secondary antibody for 1 hour at room temperature. The blots were rinsed 3 times again after which ECL substrate was applied to the blots. Then move into a dark room with a safe light, place covered membrane in a film cassette with protein side facing up. Place X-ray film on top of membrane, and expose for 1 minute. Exposure time can be increased to achieve optimal results, with light emission being most intense immediately after substrate incubation and significantly decreasing within 1

hour. For probing the beta actin protein control, stripping buffer was added to the same blots for 15 min at room temperature and then incubated them in beta actin primary antibody overnight. The rest of the protocol is the same as described above.

3.2.16 Reporter Gene (Luciferase) Assay

Luciferase assay was used for confirming the effect of miR-122 on the selected target gene 3'UTRs. We plated 2×10^4 293T cells or colorectal cancer cells in quadruplicate in a 96-well plate with 200µl complete medium. The next day the cells were rinsed by PBS and transfected with either miR-122 mimic or negative control miRNA together with six different plasmids respectively in serum free medium (SFM) using METAFECTENE® (Biontex) transfection reagent. All miRNA mimics, inhibitors and corresponding negative controls were purchased from Ambion. Each well was transfected with 50nM miRNA or control miRNA, 100ng of 3' UTR plasmid construct and 20ng of Firefly luciferase vector. 24 hours after the transfection, the cells were washed with PBS. After complete aspiration of the PBS, the Dual-Luciferase® Reporter Assay System from Pro mega was used as follows: 20µl of 1×passive lysis buffer was added to each well and the plate was placed on rotary shaker for 15 min at room temperature. Subsequently, 50µl of LAR was added and the Firefly luciferase activity was measured luciferase activity on the Infinite M200 Microplate reader (Tecan) machine. Then 50µl of freshly constituted Stop & glo added and the Renilla luciferase activity was measured. The luciferase activity (Renilla/Firefly) in each well for each given UTR was calculated and the relative luciferase activity was obtained by normalizing to the corresponding control.

3.2.17 Exosome isolation

The exoEasy Maxi Kit was used for purifying exosomes from up to 16 ml of cell culture supernatant. Huh7 was cultured in normal DMEM media to 60-70% confluency. The cells were washed by PBS and serum free DMEM media was added. 2 days later, the media was collected and centrifuged for 30 min. 1 volume buffer XBP (from the kit) was added to 1 volume of supernatant. The combination was mixed by gently inverting the tube 5 times. The sample/XBP mix was then added onto the exoEasy spin column and centrifuged at 500 x g for 1 min. The flow-through was then discarded followed by the addition of 10 ml of buffer XWP and centrifugation at 5000 x g for 5 min. After discarding the flow-through, the spin column was transferred to a fresh collection tube. 400 µl Buffer XE was added to the membrane and allowed to sit for 1 min. The column was then centrifuged at 500 x g for 5 min to collect the eluate. The eluate was re-applied to the exoEasy spin column membrane and allowed to sit for

1 min and centrifuged again at 5000 x g for 5 min to collect the eluate. The exosome containing eluate was stored at -20°C.

The exoRNeasy Serum/Plasma Starter Kit was used for purification of total exosome-derived RNA. After the addition of 1 volume Buffer XBP to 1 volume of the supernatant and mixing as described earlier, the sample/Buffer XBP mix was added onto the exoEasy spin column and centrifuged for 1 min at 500 x g. The flow-through was discarded followed by the addition of 10 ml Buffer XWP and centrifugation for 5 min at 5000 x g to wash the column. The flow-through was discarded and the spin column transferred to a fresh collection tube. 700 µl QIAzol reagent was added to the membrane and spun for 5 min at 5000 x g to collect the lysate which was transferred to a new microfuge tube. This tube was briefly vortexed and incubated at room temperature (15–25°C) for 5 min after which 90µl chloroform was added and shaken vigorously for 15 s. After 2–3 min of incubation, the tube was centrifuged at 12,000 x g and 4°C for 15 min. The upper aqueous phase was transferred to a new collection tube. 2 volumes of 100% ethanol were added and mixed thoroughly by pipetting. The sample was transferred to an RNeasy MinElute spin column and RNA was isolated as described above. The concentration of RNA was measured by NanoDrop™ 2000 Spectrophotometer (ThermoFisher).

3.2.18 Cell proliferation assay

Cell proliferation was determined with CellTiter 96® AQueous One Solution Reagent which contained a novel tetrazolium compound [3-(4, 5-dimethylthiazol-2-yl)-5-(3-carboxymethoxyphenyl)-2-(4-sulfophenyl)-2H-tetrazolium, inner salt; MTS (a)] and an electron coupling reagent (phenazine ethosulfate; PES). RKO, HCT116 and DLD1 cell lines were transfected with miRNA mimics, inhibitors or corresponding controls. 24 hours later, Cells were seeded in 96-well plates at a density of 2×10^3 cells/well in a total volume of 100 µl of medium with 10% FBS. Six replicates were made for each condition and each evaluated time point. 20 µl of CellTiter 96 was added to each well and the absorbance was measured using a microplate reader (TECAN Trading AG, Switzerland) at 490 nm over a period of 96 - 120 hours.

3.2.19 Colony formation assay

RKO and HCT116 cells were transected with miRNA mimics, inhibitors or their corresponding controls. 16–18 hrs after transfection, cells were trypsinized and re-seeded at a

density of 400–600 cells/well in a 6 well plate and maintained in their corresponding media containing 10% FBS at 37 °C. After 7-10 days, the colonies could be watched by eyes. Then the cells were fixed with methanol and stained with 0.1% crystal violet for 15 min. The ensuing colonies were scanned and counted by ImageJ.

3.2.20 Cell cycle assay

The cell cycle was assessed using the propidium iodide assay followed by flow cytometric analysis. RKO, HCT116 and DLD1 Cells RKO and HCT116 cells were transected with miRNA mimics, inhibitors or their corresponding controls. Cells were trypsinized 48h after transfection, washed with PBS, fixed in 1 ml cold 70% ethanol (1×10^6 per ml), and incubated at -30 °C for at least 1 hour. Next cells were washed with 10ml PBS again, resuspended in 1ml PBS, added RNase (final concentration 50 µg/ml) and incubated 30 minutes at 37 °C in the dark. Then cells were stained with propidium iodide (50 µg/ml) (Sigma-Aldrich Corp. Saint Louis, MO, USA) and analyzed by Fluorescence-activated cell sorting (FACS). The data obtained were analyzed using the FlowJo v10 software.

3.2.21 Statistical Methods

The differences between groups were statistically analyzed using two tailed unpaired and paired t-tests when dealing with independent (cell lines, before/after treatment) and dependent (tumor/normal patient) variables respectively. All experiments were carried out at least in triplicate and at least in three independent attempts. Calculations were made using Microsoft Excel. Data were considered to be statistically significant when $p < 0.05$ and represented graphically as $p < 0.05$ (*) and $p < 0.01$ (**).

4 RESULTS

4.1 Metastasis associated genes are predicted targets of miR-122

We used a combination of methods to explore putative novel oncogenic target mRNAs for miR-122. In the first approach, we looked for targets of miR-122 that had in one way or the other being implicated in metastasis. Through this function-based approach, *RIMS1* and *RABL6/C9orf86* were identified as the most significant hits. In the second approach, we pooled all of the predicted targets and put them into a pathway analysis tool. Using the Ingenuity Pathway Analysis (IPA) package, we identified and selected the Integrin pathway, which featured prominently in the output of significant pathways. The integrin pathway plays important roles in cancer invasion and metastases. The miR-122 targets in this pathway were *ABL1*, *GIT1*, *GRB7*, and *ITGAL*. The alignments of these 6 genes with miR-122 are shown in Figure 5.

hsa-miR-122/ABL1 Alignment		
3' guuUGUGGUA-ACAG-UGUGAGGu 5' hsa-miR-122 : :	mirSVR score: -0.0006 PhastCons score: 0.3754	
448:5' gucAGGCCUCUGCCUGCACUCCc 3' ABL1		
hsa-miR-122/ABL1 Alignment		
3' guuugugguaacaguGUGAGGu 5' hsa-miR-122 	mirSVR score: -0.0017 PhastCons score: 0.3997	
978:5' gcccuccccucccccCACUCCu 3' ABL1		
hsa-miR-122/C9orf86 Alignment		
3' guUUGUGGUAACAG--UGUGAGGu 5' hsa-miR-122 : : :	mirSVR score: -0.5329 PhastCons score: 0.5086	
610:5' gaGGCACUCCUCCCAAACACUCCa 3' C9orf86		
hsa-miR-122/C9orf86 Alignment		
3' guuUGUGGUAACAGUGUGAGGu 5' hsa-miR-122 :	mirSVR score: -0.1137 PhastCons score: 0.5086	
634:5' cucAGACCA-UAAAGCACUCCu 3' C9orf86		
hsa-miR-122/GRB7 Alignment		
3' guuugugguaacaguGUGAGGu 5' hsa-miR-122 	mirSVR score: -0.0081 PhastCons score: 0.4849	
106:5' gcgggagggguuccgcCACUCCa 3' GRB7		
hsa-miR-122/GRB7 Alignment		
3' guuugugguaacaguGUGAGGu 5' hsa-miR-122 	mirSVR score: -0.0060 PhastCons score: 0.4987	
169:5' gccccacuccagucCACUCCu 3' GRB7		
hsa-miR-122/GRB7 Alignment		
3' guuugugguaacaguGUGAGGu 5' hsa-miR-122 	mirSVR score: -0.0094 PhastCons score: 0.4918	
159:5' auagaaaacagccccCACUCCa 3' GRB7		

hsa-miR-122/GIT1 Alignment		
3' guuuGUGGUAACAGUGAGGGu 5' hsa-miR-122 : ::	mirSVR score: -0.0774 PhastCons score: 0.6309	
106:5' ccuUAGUGCUGCCACACUCCc 3' GIT1		
hsa-miR-122/GIT1 Alignment		
3' guuuguggUAACAGUGAGGGu 5' hsa-miR-122 :	mirSVR score: -0.1246 PhastCons score: 0.6089	
315:5' aggggcagGUGGGGACACUCCa 3' GIT1		
hsa-miR-122/GIT1 Alignment		
3' guuugugguaacaguGUGAGGGu 5' hsa-miR-122 	mirSVR score: -0.0047 PhastCons score: 0.6054	
44:5' ccuaggagcugggcCACUCCa 3' GIT1		
hsa-miR-122/GIT1 Alignment		
3' guuugugguaacaguGUGAGGGu 5' hsa-miR-122 	mirSVR score: -0.0015 PhastCons score: 0.6089	
262:5' gggccugcaaggcauCACUCCc 3' GIT1		
hsa-miR-122/RIMS1 Alignment		
3' guuUGUGGUAAC-AGUGAGGGu 5' hsa-miR-122 :: :	mirSVR score: -1.0265 PhastCons score: 0.5905	
883:5' auuGUACU-UUGAAAACACUCCu 3' RIMS1		
hsa-miR-122/RIMS1 Alignment		
3' guuugUGGU-AACAG---UGUGAGGGu 5' hsa-miR-122 	mirSVR score: -1.0362 PhastCons score: 0.8189	
1999:5' uuuugACCACUUGUCUUAACACUCCc 3' RIMS1		
hsa-miR-122/ITGAL Alignment		
3' guuuGUGGUAACA-GUG-UGAGGGu 5' hsa-miR-122 	mirSVR score: -0.3221 PhastCons score: 0.5188	
751:5' cuucCACCAGCCUGCACUACUCCc 3' ITGAL		
hsa-miR-122/ITGAL Alignment		
3' guUUG--UGGUAACAGUGAGGGu 5' hsa-miR-122 ::	mirSVR score: -0.0507 PhastCons score: 0.5557	
377:5' agAACCUUGUCCUUG-CACACUCCc 3' ITGAL		
hsa-miR-122/ITGAL Alignment		
3' guuUGUGGUAACAGUGAGGGu 5' hsa-miR-122 : : :	mirSVR score: -0.0020 PhastCons score: 0.5082	
1234:5' auuGCGCAU---GCACUCCa 3' ITGAL		

Figure 5. The alignments of these 6 genes with miR-122.

Retrieved from: <http://www.microrna.org>

4.2 Amplification and cloning of 3' UTRs in pLightSwitch 3' UTR Vector

To determine if these 6 genes were direct targets of miR-122, we first of all amplified the 3' UTRs of *RIMS1*, *RABL6/C9orf86*, *ABL1*, *GIT1*, *GRB7*, and *ITGAL* from the genomic DNA of the human embryonic kidney 293T cell lines with PCR. The amplified fragments were

resolved on an agarose gel to find out if the correct fragment size(s) had been amplified (**Figure 6**). After digestion of the fragments with *NheI* and *XhoI* and ligation in the pLightSwitch 3'UTR plasmid, several colonies were picked and a colony PCR was done with pLightSwitch specific primers to identify the clones with the correct size of insert and orientation (**Figure 7**). The clones containing the right size of insert were Sanger-sequenced to confirm the insert.

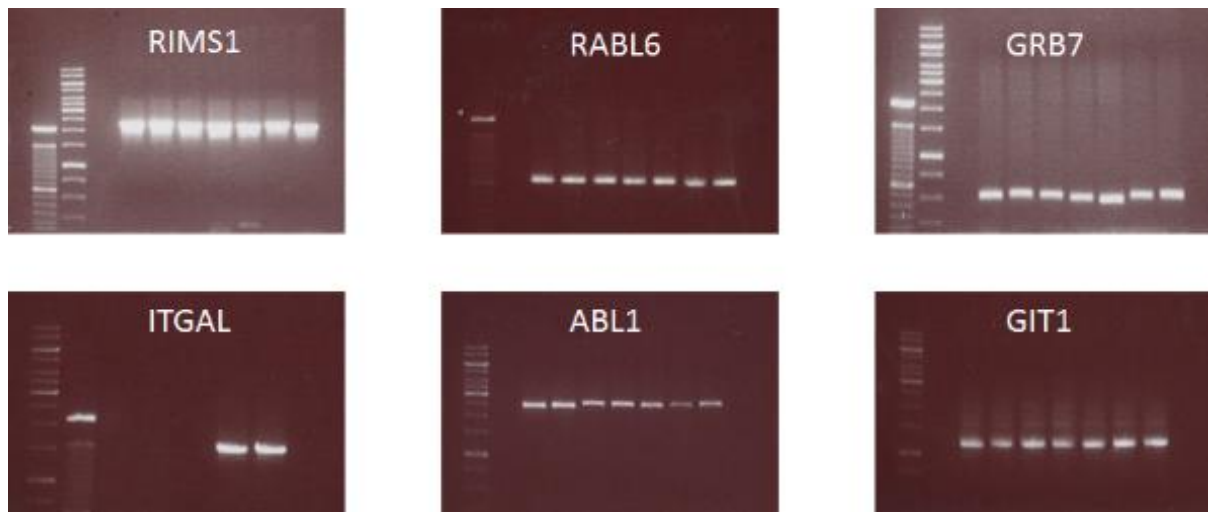


Figure 6. Agarose gel electrophoresis of PCR products of *ABL1*, *RABL6/C9orf86*, *GRB7*, *RIMS1*, *ITGAL*, and *GIT1*.

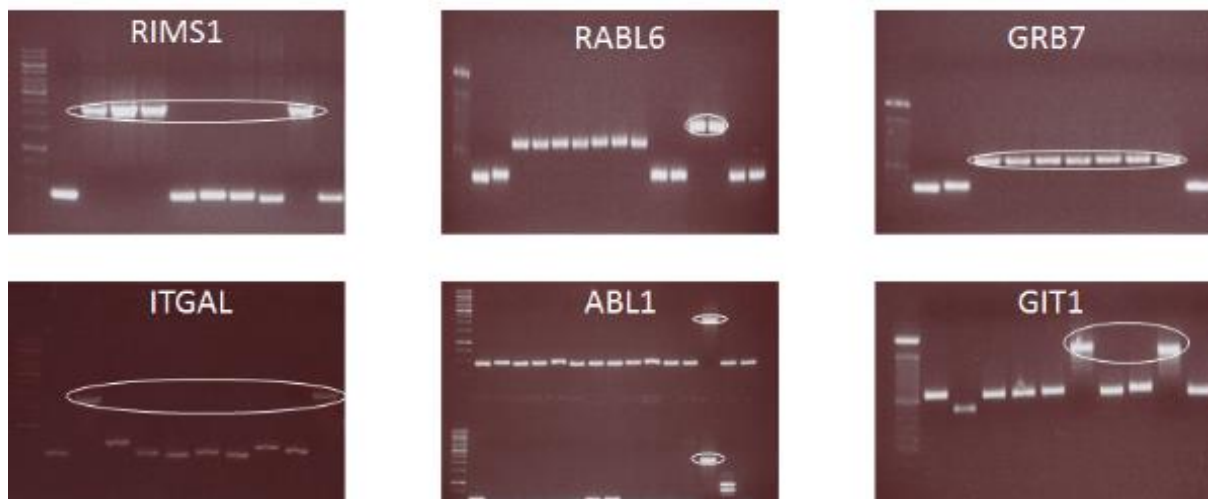


Figure 7. Agarose gel electrophoresis of colony PCR for the identification of potentially correct clones.

4.3 3' UTR Reporter gene assay identifies *RABL6* and *RIMS1* as significantly suppressed targets

The cloned plasmids of all 6 3'UTRs were subjected to a reporter gene assay in 293T, RKO, SW480 and HT1080 cells transfected with a miR-122 mimic or corresponding control. Of the 6 mRNAs, those of *RIMS1* and *RABL6* showed the most significant suppression in the presence of miR-122. Compared with the control miRNA, miR-122 significantly decreased the luciferase activity by 70.7 % in 3' UTR of *RIMS1* and 61.7% in *RABL6* in 293T cells, which means miR-122 interacts with the 3' UTR of *RIMS1* and *RABL6* (**Figure 8**). Similar results were obtained with RKO, SW480 and HT1080 cells. *GRB7* showed some mild suppression, but no suppression was seen with *GIT1*, *ABL1* and *ITGAL* (**Figure 8**).

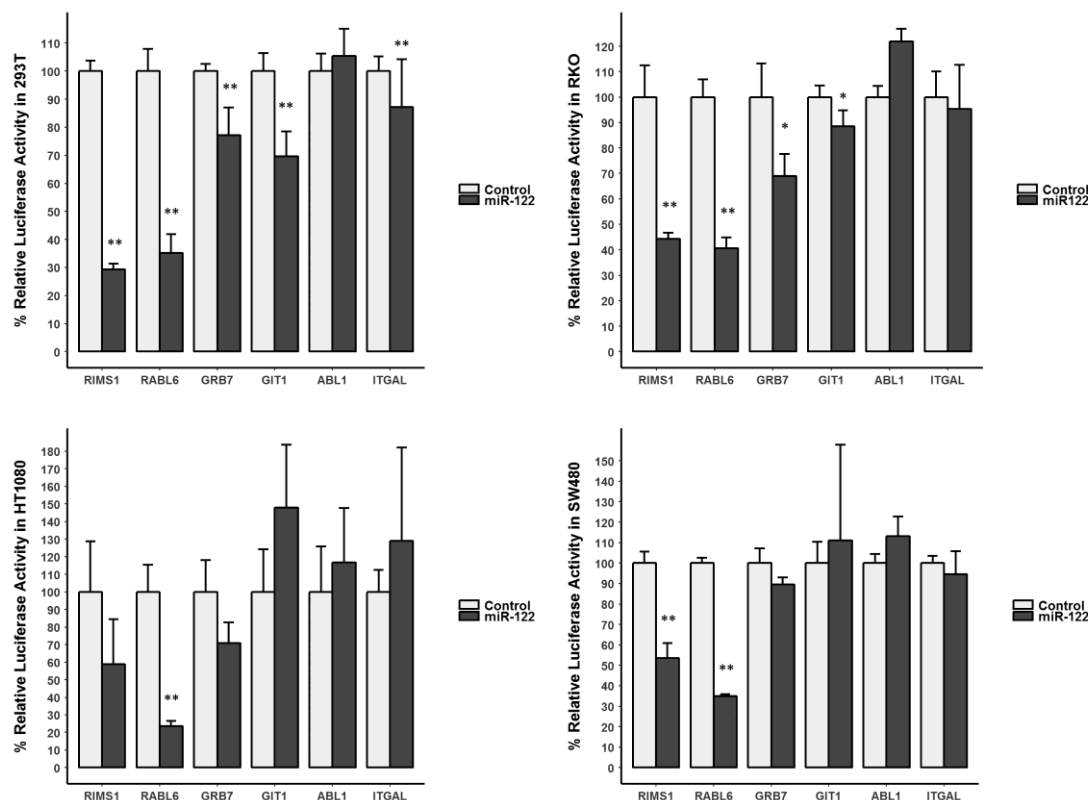


Figure 8. 3' UTR relative luciferase activity of 6 potential target mRNAs following treatment with miR-122.

4.4 Endogenous expression of miR-122 in colorectal and liver cell lines

In order to determine which cell lines would be best suited for the evaluation of miR-122 function, as well as over-expression and knock-down studies, we screened a panel of colorectal and liver cell lines for the endogenous expression of miR-122. The miR-122

expression was generally low in all the colorectal cancer cell lines screened. However, DLD1, SW480 and Caco2 showed the highest relative expression, while HT29, SW48 and SW620 showed the lowest expression levels (**Figure 9**). Since miR-122 was shown to be highly expressed in hepatocytes, we decided to analyze its expression in two hepatocellular carcinoma cell lines (Huh7 and Hep3B). While the expression of miR-122 was low in Hep3B cells, it was very highly expressed in Huh7 cells (**Figure 10**).

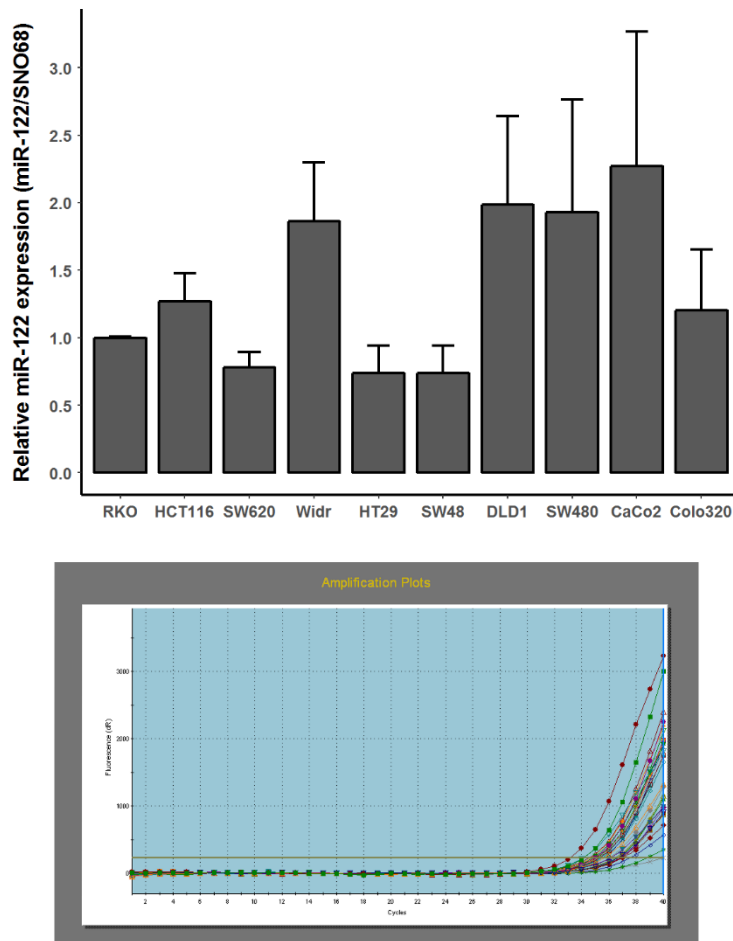


Figure 9. Cell line screening for the expression of miR-122 in a panel of colorectal cancer cell lines, graph shows expression relative to the RKO cell line after normalization to SNO68.

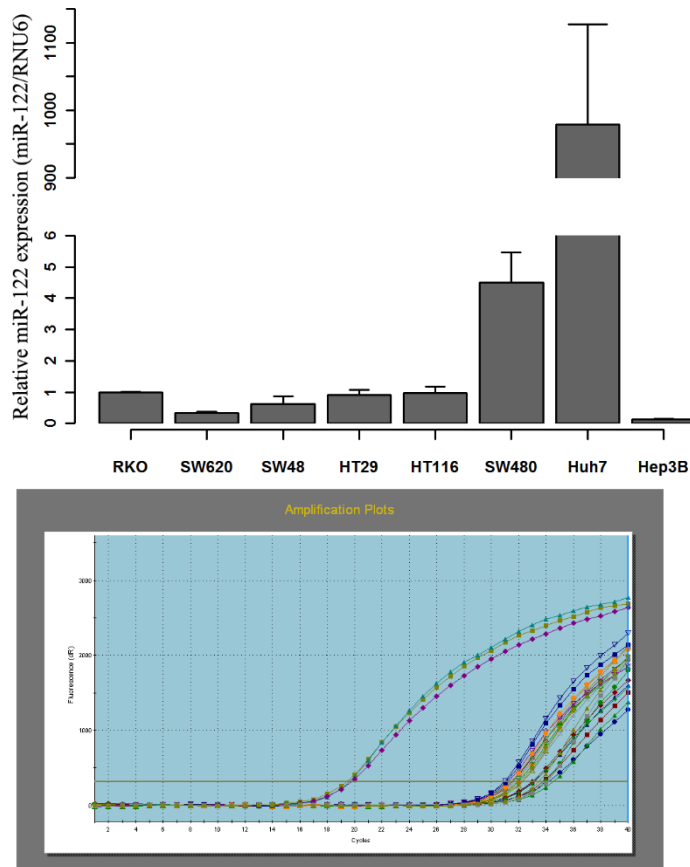


Figure 10. Cell line screening for the expression of miR-122 in colorectal cancer cell lines and 2 hepatocarcinoma cell lines, graph shows expression relative to the RKO cell line after normalization to RNU6.

4.5 miR-122 suppresses mRNA and protein expression of *RABL6* and *RIMS1*

To confirm the effect of miR-122 on the suppression of *RIMS1* and *RABL6* expression, we transfected RKO, DLD1 and HCT116 cells with miR-122 mimic or corresponding control. On the mRNA level, miR-122 led to a significant decrease of *RIMS1* ($P = 0.036348821$) and also a trend of *RABL6* decrease in RKO (**Figure 11**). Meanwhile there is a significant decrease of *RABL6* in DLD1 ($P = 0.003768173$) although no decrease of *RIMS1* (**Figure 11**). On the protein level by Western Blot, miR-122 also led to a decrease of *RABL6* expression (**Figure 12**). Based on these results, we sought to demonstrate that these two genes are direct targets of miR-122.

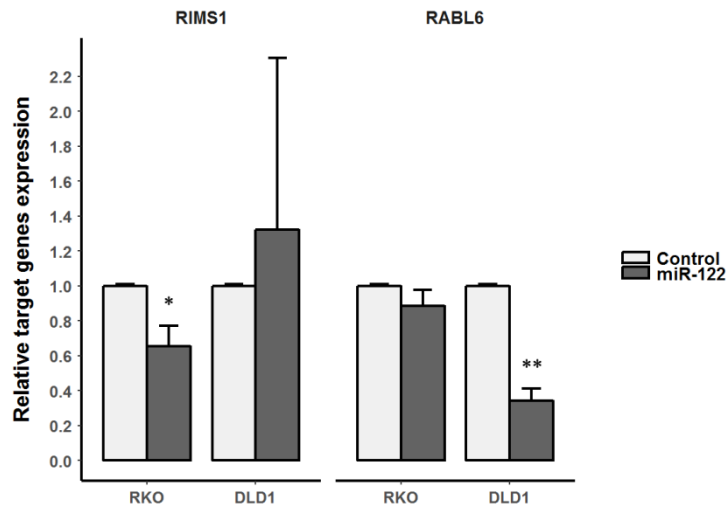


Figure 11. *RIMS1* and *RABL6* mRNA expression following transfection with miR-122 in RKO & DLD1 cell lines.

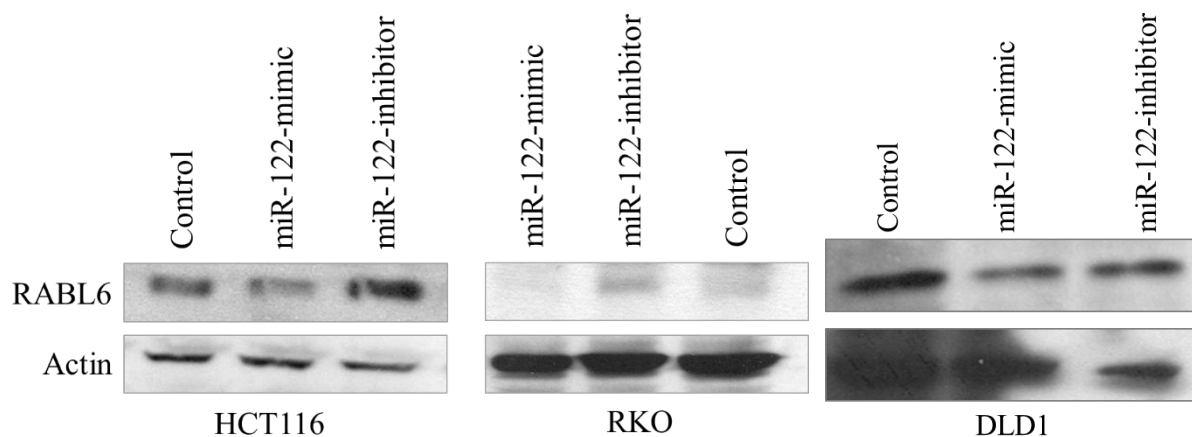


Figure 12. Assessment of *RABL6* protein expression in RKO, HCT116 and DLD1 cells following transfection with miR-122 mimic, miR-122 inhibitor and oligonucleotides.

4.6 miR-122 is secreted in the conditioned media and exosomes of Huh7 cells

We hypothesized that since the metastatic lesions were in the liver, that miR-122 was acquired by the colorectal cancer cells from the liver parenchymal cells through paracrine activity. To prove this hypothesis, we analyzed the conditioned media of Huh7 cells for miR-122 abundance relative to control serum free media. Additionally, we checked to see if any extra-cellular miR-122 was present in the exosomal fraction of the conditioned media. RNAs were purified from conditioned media (no FBS DMEM media) of Huh7 cells as previously

described. From 16 ml media, the RNA concentration was about 150ng/ μ l compared to 0ng/ μ l in fresh media. Real-time PCR was used to amplify miR-122 in total exosomes (**Figure 13**).

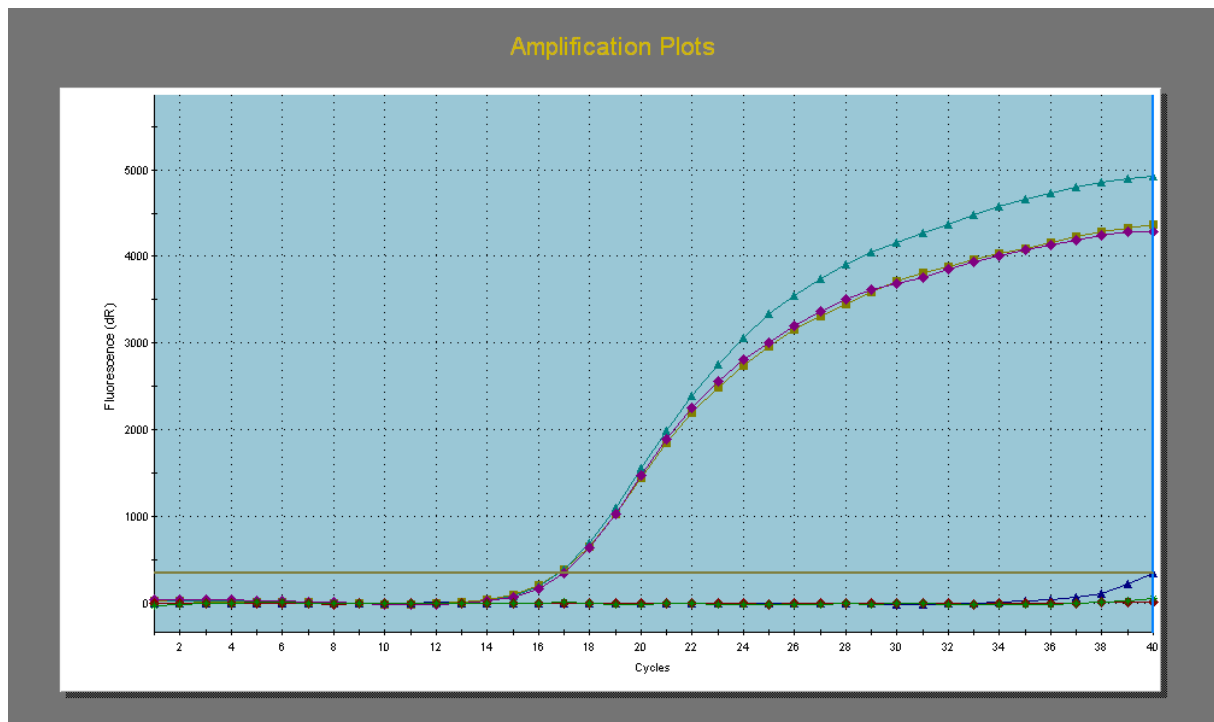


Figure 13. The expression of miR-122 in exosomes extracted from conditioned media of Huh7 cells.

4.7 Huh7 Liver cancer cells are able to transfer miR-122 to colorectal cancer cells in co-culture, through conditioned media and exosomes

After confirming that miR-122 was secreted into the conditioned media and was present in exosomes, we proceeded to find out if these miRs could be taken up by colorectal cancer cells, in a situation similar to what we had observed in the patient samples. Towards this end, Huh7 cells were cultured with RKO cells (Huh7 cells were plated 2 days before RKO cells as described in 2.2.2). After 3-5 days of co-culture, total RNA from RKO cells in the top well was collected and real-time PCR was performed to measure miR-122 expression. From the third day, we observed an increase of miR-122 expression in RKO cells. Moreover, this expression was still significantly enhanced on the fourth day and fifth day relative to control cells (**Figure 14**), which means RKO cells could take up miR-122 secreted from Huh7 cells.

To further confirm that this transfer was from exosomes, we directly added the exosomes extracted from conditioned media of Huh7 into normal medium of RKO and HCT116 cells,

using the buffer for exosomes in the kit as the negative control. The miR-122 expression was significantly upregulated in RKO however only a slightly upregulated in HCT116 (**Figure 15**).

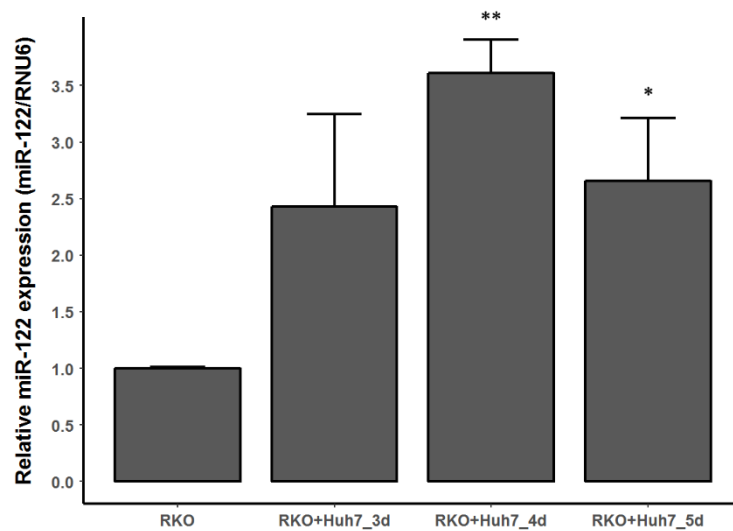


Figure 14. The expression of miR-122 in the RKO cell line co-cultured with the Huh7 cell line after 3 days, 4 days and 5 days.

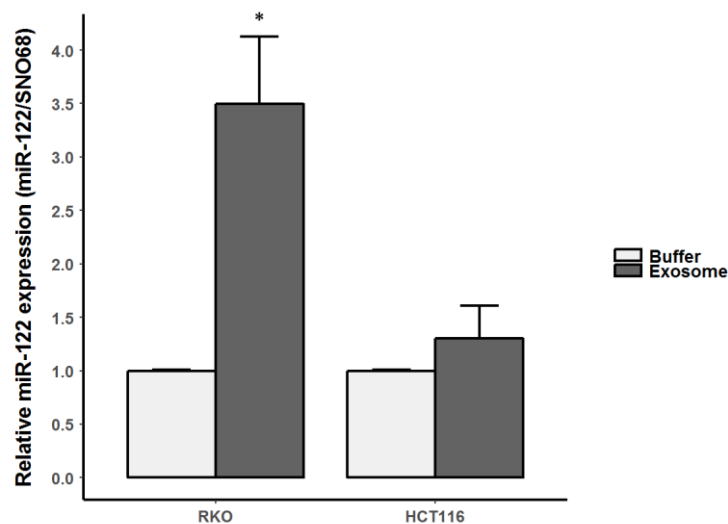


Figure 15. The expression of miR-122 in RKO & HCT116 cells treated with exosomes extracted from Huh7 conditioned media. Exosome elution buffer was used as a negative control.

4.8 Liver cell exosomes mediate suppression of target genes in colorectal cancer cell lines

To further confirm if *RIMS1* and *RABL6* could be targeted by miR-122 from exosomes, we directly added exosomes extracted from conditioned media of Huh7 into normal medium of

RKO, HCT116 and DLD1 cells, and the exosome elution buffer as a negative control. On the mRNA level, miR-122 led to a significant decrease of *RIMS1* in all three cell lines and a significant decrease of *RABL6* in RKO and DLD1 cells. Moreover, we also observed a trend of decreased expression of *RABL6* in HCT116 (Figure 16).

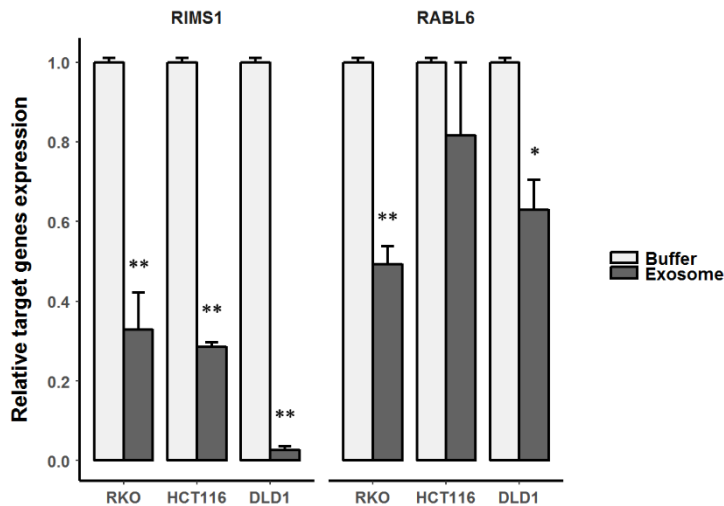


Figure 16. *RIMS1* and *RABL6* mRNA expression in RKO, HCT116 & DLD1 cell lines following treatment with exosomes extracted from Huh7 cell conditioned media. Exosome elution buffer was used as a negative control.

4.9 Cell cycle genes are downstream effectors of *RABL6* and are suppressed by miR-122

Since *RIMS1* and *RABL6* expression could be suppressed by miR-122 in colorectal cancer cell lines, we tried to assess the effects of miR-122 not only on its direct targets, but also on related signaling molecules. Although there are few reports about *RIMS1*, the cumulative data suggests that *RABL6* might be an important regulator for cell proliferation and G1-S transition (Hagen et al., 2014; Tang et al., 2016). We also found miR-122 upregulated cyclin-dependent kinase inhibitor 1A (CDKN1A, P21) expression in both RKO and HCT116 cell lines (Figure 17), which is a classical cell cycle checkpoint inhibitor protein. These results suggest that miR-122 induced suppression of *RABL6* caused P21 upregulation.

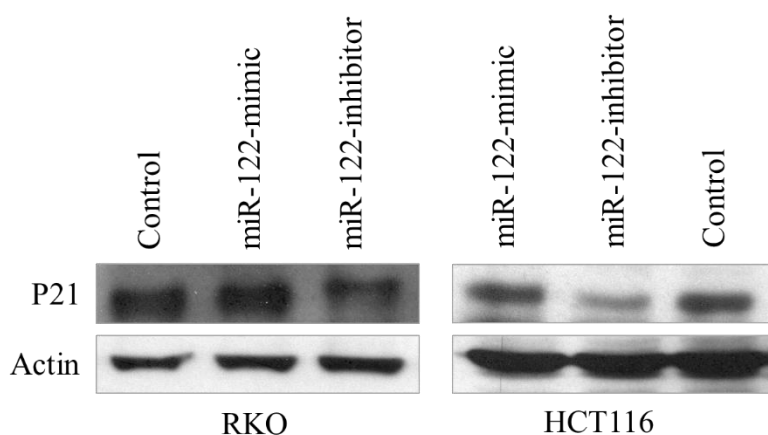


Figure 17. Assessment of P21 protein expression in RKO and HCT116 cells following transfection with miR-122 mimic, miR-122 inhibitor and oligonucleotides.

4.10 Targeting of *RIMS1* and *RABL6* suppresses tumor cell proliferation and colony formation

To explore the function of *RIMS1* and *RABL6*, RKO, HCT116 and DLD1 cells transfected by miR-122 and its inhibitor were subjected to cell proliferation and colony formation assays. The cell proliferation assay was evaluated over a 4 or 5-day time period. Although there was no significant difference in RKO cells, we observed a significant decrease in cell proliferation in HCT116 and DLD1 cells in which miR-122 had been over-expressed, and a corresponding increase in HCT116 cell with miR-122 inhibitor (**Figure 18**). Additionally, RKO, HCT116 and DLD1 cells transfected by miR-122 and its inhibitor were analyzed by flow cytometry. We observed that a slightly higher amount of cells transfected with miR-122 arrested in the G0/G1 phase comparing to controls nearly in all cell lines at both 48h and 72h except in HCT116 at 72h (**Figure 19**). These results suggested a potential role for miR-122 in regulating the G1/S transition by targeting *RABL6* and regulating P21.

Similarly, colony formation assays showed significantly fewer colonies with the transfection of miR-122 mimics compared to controls in both RKO and HCT116 cells (**Figure 20**). The converse was observed with the miRNA inhibitors. This result further supports miR-122 as an inhibitor of cell proliferation by suppressing *RABL6* expression.

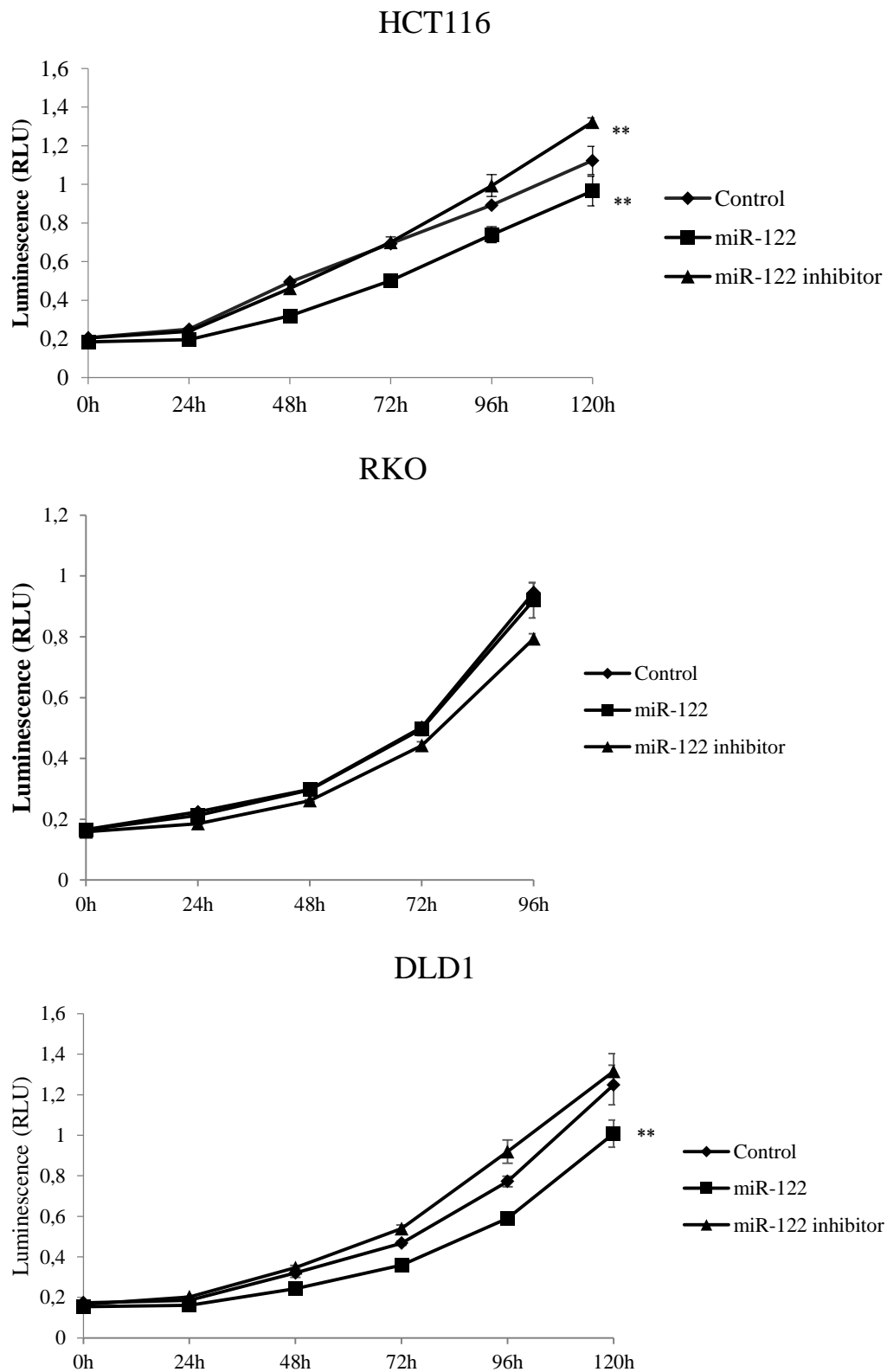


Figure 18. Cellular growth curves of RKO, HCT-116 and DLD1 cell lines at 24 hours following transfection with miR-122 mimic, miR-122 inhibitor or control oligonucleotides.

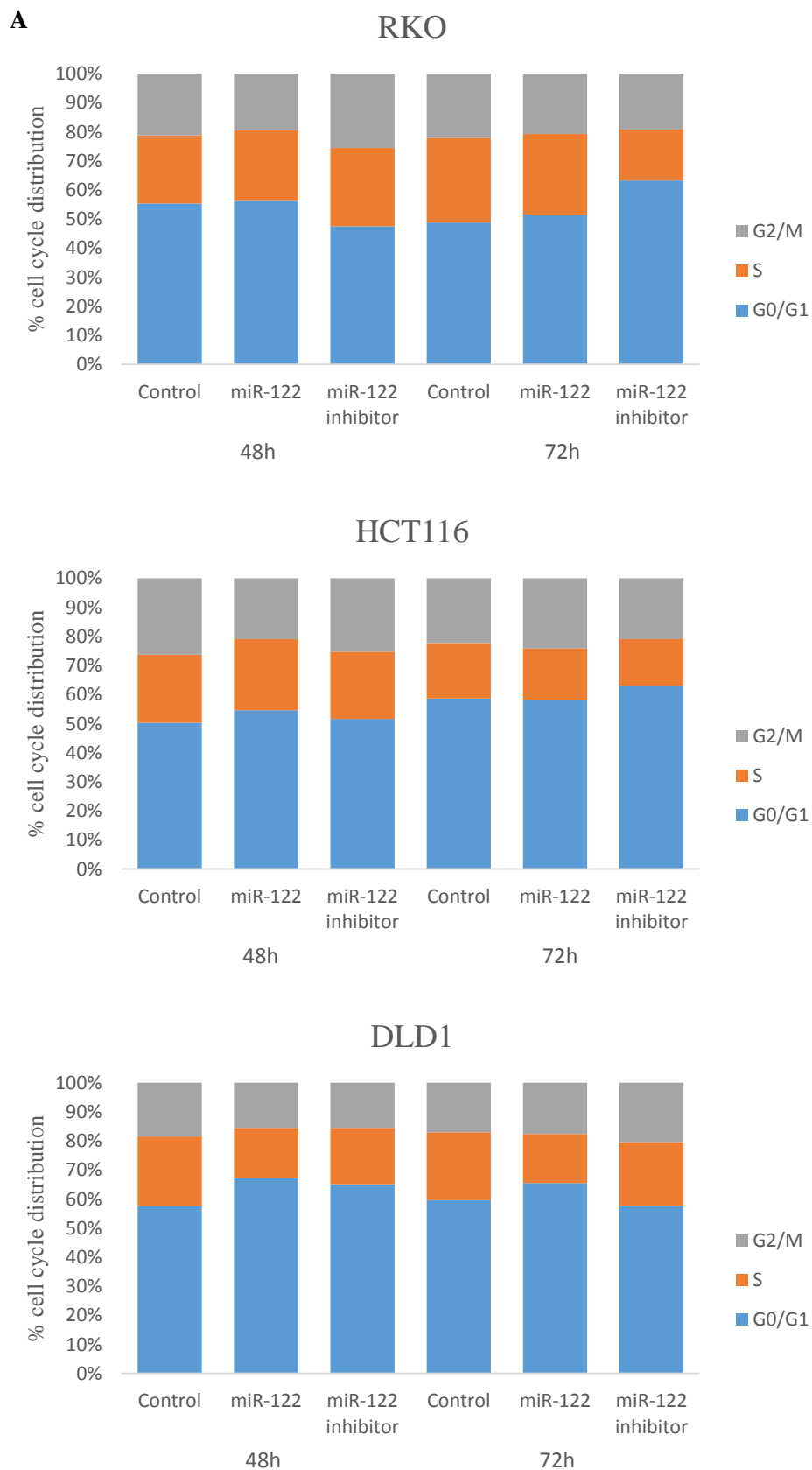


Figure 19 (A). Cell cycle analysis of RKO, HCT116 and DLD1 cells transfected with miR-122 mimics, inhibitors or corresponding controls. The graph shows the relative percentages of cells in the

different phases of the cell cycle (G0/G1 vs S vs G2/M) and how these are affected by miR-122 mimic and inhibitor treatment.

B		Control	miR-122	miR-122 inhibitor
48h	%G0/G1 RKO	55.4%	56.2%	47.6%
	%G0/G1 HCT116	50.2%	54.6%	51.6%
	%G0/G1 DLD1	57.6%	67.2%	65.1%
72h	%G0/G1 RKO	48.8%	51.6%	63.3%
	%G0/G1 HCT116	58.6%	58.2%	62.9%
	%G0/G1 DLD1	59.6%	65.5%	57.7%

Figure 19 (B). Tabular representation of the cell cycle analysis in RKO, HCT116 and DLD1 cells transfected with miR-122 mimics, inhibitors or corresponding controls. The percentage of cells in G0/G1 phase is increased by the miR-122 mimic.

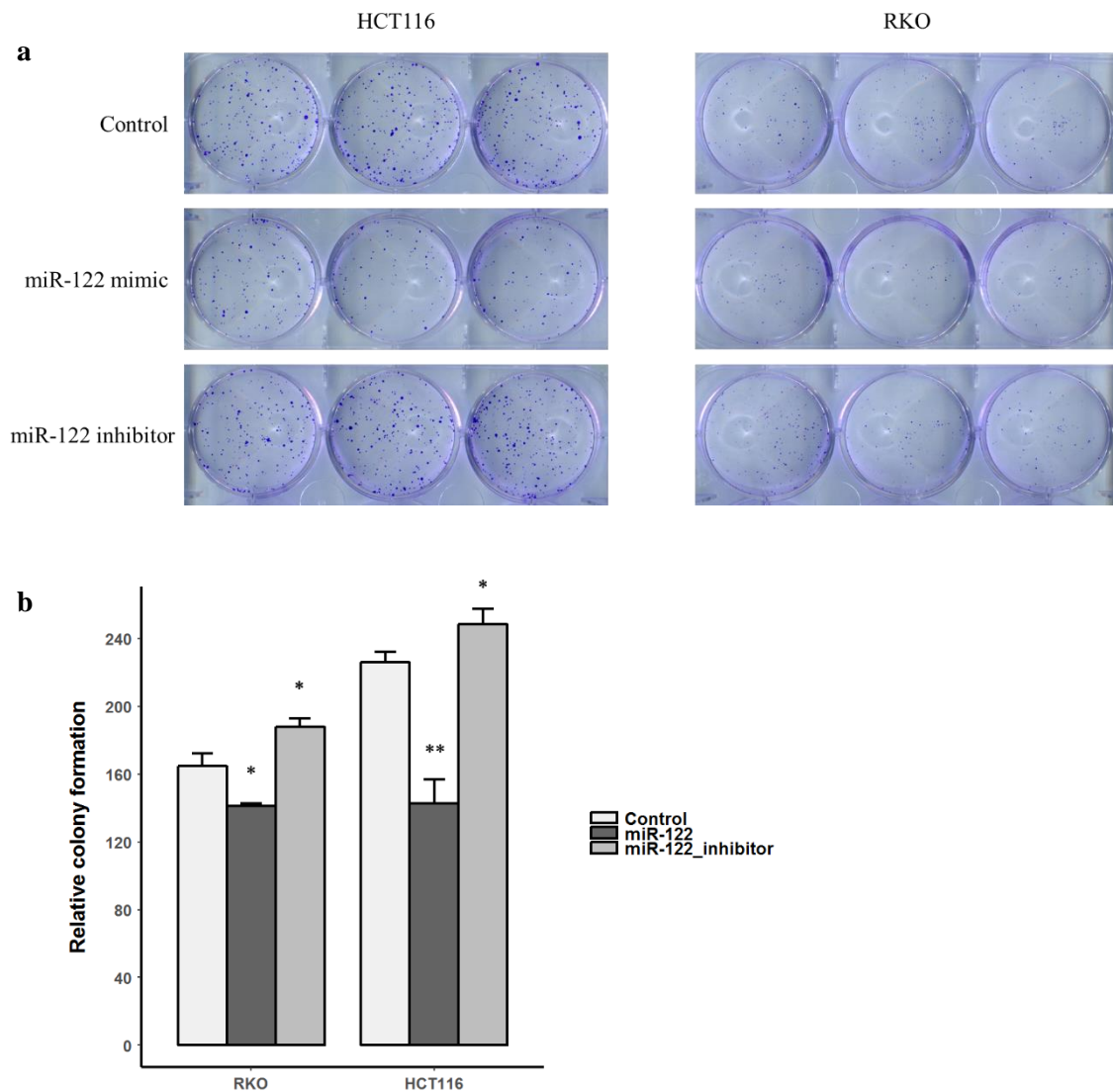


Figure 20. Colony formation assays performed with RKO and HCT116 cells. The cell lines were treated with miR-122 mimics, inhibitors or corresponding controls. **(a)** Representative examples of the scanned plates. **(b)** Overall quantification of the colonies conducted in ImageJ. Details are as described in the Materials and Methods.

4.11 Targeting of RIMS1 and RABL6 might not affect tumor cell migration and invasion

Since *RABL6* and *P21* were identified as important regulators for cell proliferation and G1-S transition, we also wanted to know if they could affect tumor cell migration or invasion. RKO, HCT116 and DLD1 cells transfected by miR-122 and its inhibitor were subjected to cell migration or invasion assays. Unfortunately, there was only one significant case of DLD1

cells enhancing invasion following miR-122 inhibitor transfection (**Figure 21**). There was no significant difference in other cells.

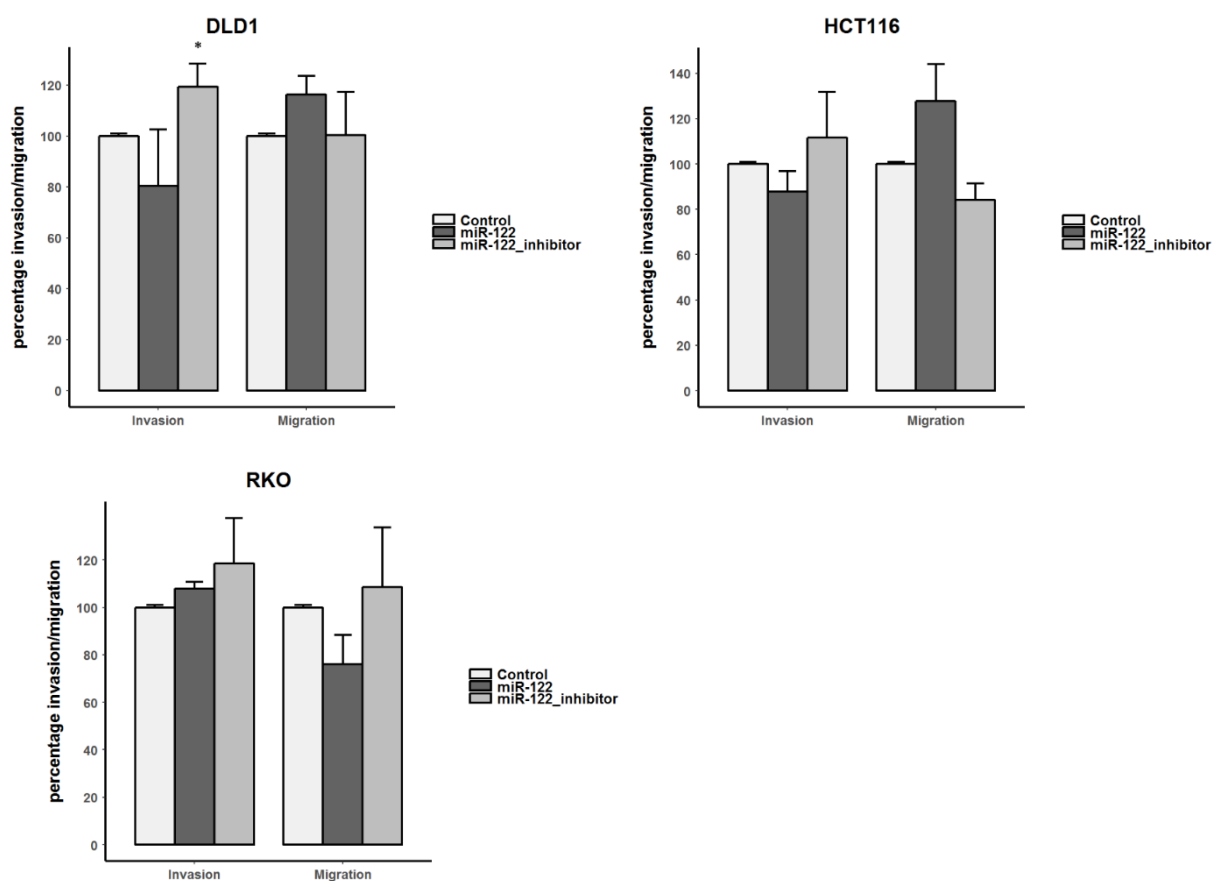


Figure 21. Invasion and migration assays in DLD1, HCT116 and RKO cells transfected with miR-122 mimics, inhibitors or corresponding controls.

5 DISCUSSION

Metastasis continues to be the major factor impacting prognosis and survival of colorectal cancer patients. Metastasis itself is not a single process but rather, a constellation of multiple events that culminate with the colonization of distant sites by the primary tumor. A number of published reports seem to indicate that the events playing in different metastatic sites are not identical and every metastatic niche is inherently different. In colorectal cancer, as well as several other solid tumors, the liver is a common site for metastasis. Decrypting novel molecular regulators modulating CRC metastasis will help to further understand CRC biology, and may provide potentially efficient targets for CRC therapy.

The adaptation of tumor cells to a foreign microenvironment is critical to successful metastatic colonization (McGowan, Kirstein, & Chambers, 2009; Peinado, Lavotshkin, & Lyden, 2011; Talmadge & Fidler, 2010). This has been described as a highly inefficient process with circulating tumor cells trying to overcome many obstacles to colonize distant organs. These events include infiltrating distant tissue, evading immune defenses, adapting to supportive niches, surviving as latent tumor-initiating seeds and eventually breaking out to replace the host tissue (Massague & Obenauf, 2016). Despite immune defenses, there are some supportive niches that cancer cells can benefit from. Evidence exists that primary tumors can send systemic signals to influence the microenvironment of distant organs by creating pre-metastatic niches before the arrival of cancer cells (McAllister & Weinberg, 2014).

After colonization, most metastasized cells enter a state of dormancy, of which two modes have been described. Tumor mass dormancy, in which micrometastases stop growing because of insufficient vascularization or constant culling by immune defenses; and cellular dormancy, where isolated disseminated tumor cells enter a proliferative quiescence state (Sosa, Bragado, & Aguirre-Ghiso, 2014). Which of the two modes is more frequent is uncertain (Strauss & Thomas, 2010), but it has been postulated that DTCs might enter the cell cycle intermittently, and undergo rapid elimination by the immune system. But in the end, some progeny will evolve the ability to escape immune defenses and develop overt metastatic lesions. There is increasing evidence suggesting that microRNAs are major players in all the steps of the metastasis cascade.

miRNAs are important metastasis molecules

In an effort to better understand the molecular events at play in colorectal cancer liver metastasis, Prof. Allgayer's department sequenced the whole genomes of 12 patients with advanced colorectal cancer. Other studies have also compared different primary tumors with their corresponding metastasis in the search for molecular mediators of metastasis, but in most cases looking for specific miRNAs or sequences. In some these studies, the pattern of some miRNA expression could distinguish primary tumors from their corresponding metastases, confirming a direct involvement of miRNAs in cancer metastasis, e.g. miR-10b, miR-21, miR-30a, miR-30e, miR-125b, miR-141, miR-200b, miR-200c, and miR-205 (Baffa et al., 2009). In several studies, including work of the Allgayer team, a number of miRNAs were found to participate in different processes of metastasis by modulating the expression of genes involved in metastasis-related pathways and signaling networks, such as the phosphatase and tensin homolog (PTEN)/phosphatidylinositol-3-kinase (PI3K), EGF receptor (EGFR), TGF β , and p53 pathways (Fish et al., 2008). In a further example, the loss of miR-200c expression was found to induce an aggressive, invasive, and chemoresistant phenotype by repressing E-cadherin in non-small lung cancer (Ceppi et al., 2010).

Interestingly, increasingly more key signaling pathways implicated in metastatic colon cancer that are targeted by microRNAs, are being identified. For instance, EGFR, a receptor tyrosine kinase (RTK) has been shown to be involved in CRC progression and metastasis, and a handful of anti-EGFR agents, including tyrosine kinase inhibitors (TKIs) and monoclonal antibodies against EGFR (Giampieri et al., 2013) have been developed. However, most anti-EGFR targeted agents are frequently susceptible to drug-resistance. Increasing evidence has demonstrated that certain miRNAs correlate with drug resistance to anti-EGFR agents, and depending on whether the correlation is positive or negative, inhibitors or mimics can be used. For example, a combination of miR-7 and cetuximab, a monoclonal antibody against EGFR could enhance the growth inhibitory effect as compared to each agent alone (Suto et al., 2015). A miRNA profiling analysis in metastatic colorectal cancer (mCRC) patients treated with anti-EGFR monoclonal antibodies identified the let-7c/miR-99a/miR-125b miRNA cluster as a signature associated with an outcome different from that of anti-EGFR therapies, and this miRNA cluster may be used for the selection of patients with KRAS wild-type mCRC as good candidates for anti-EGFR therapy (Cappuzzo et al., 2014). Moreover, miRs-134 and -

370 were identified as tumor suppressor miRNAs that could suppress colorectal cancer tumorigenesis by regulating the EGFR signaling cascade (El-Daly et al., 2016).

The miR-17-92 cluster is composed of six miRNAs (miR-17, -18a, -19a, -20a, -19b-1, and -92a-1) was the first to be demonstrated as oncogenic (He et al., 2005). Consistent with its oncogenic role, the miR-17-92 cluster is upregulated in a variety of cancers including lymphomas (He et al., 2005; Rinaldi et al., 2007), lung cancers (Matsubara et al., 2007), and others (Volinia et al., 2006).

miR-21 is one the most extensively studied miRNAs. It is upregulated in almost all kinds of cancers. It is transcriptionally activated by signal transducer and activator of transcription 3 (Stat3) (Loffler et al., 2007) and also by CD24 expression of via SRC (Muppala et al., 2013). miR-21 was found to promote invasion, intravasation, and metastasis by downregulating Pdc4 (Asangani et al., 2008). It also promotes cell motility and invasion by directly targeting PTEN (phosphatase and tensin homolog), a tumor suppressor known to inhibit cell invasion by blocking the expression of several matrix metalloproteases (Meng et al., 2007).

The miR-34 family (miR-34a, b and c) are induced by p53 and are downregulated in several tumors such as non-small cell lung cancers (Bommer et al., 2007) and pancreatic cancers (T. C. Chang et al., 2007). However, reduction of the miR-34s is not always correlated with p53 loss, suggesting a p53-independent mechanism of miR-34 reduction in some cancers. The oncoproteins CD24 and SRC are both downregulated by miR-34a (Muppala et al., 2013).

Recently, miR-224 expression was observed to consistently increase with tumour burden and microsatellite stable status in colorectal cancer. miR-224 was found to enhance CRC metastasis in vitro and in vivo, by directly targeting SMAD4 (Ling et al., 2016).

The APC gene is one of the first to be lost in CRC and its loss was found to trigger the overexpression of miR-135b through PTEN/PI3K pathway deregulation, and SRC overexpression resulting in tumor transformation and progression. In CRCs, miR-135b overexpression correlated with tumor stage and poor clinical outcome and the inhibition of this miRNA in CRC mouse models reduces tumor growth by controlling genes involved in proliferation, invasion, and metastasis. (Valeri et al., 2014).

Lately, miR-551a and miR-483 were identified as robust endogenous suppressors of liver colonization and metastasis. These miRNAs convergently targeted creatine kinase, brain-type (CKB), which routinely contributes to the generation of phosphocreatine. CKB is released into the extracellular space by metastatic cells encountering hepatic hypoxia and catalyzes production of phosphocreatine that is used to generate ATP, fueling metastatic survival (Loo et al., 2015).

The epithelial to mesenchymal transition is often considered as an integral step in metastasis. The hallmark of EMT is the downregulation of the E-cadherin protein. The loss of miR-200c expression was found to induce an aggressive, invasive, and chemoresistant phenotype by repressing E-cadherin in non-small lung cancer (Ceppi et al., 2010). Also, miR-30a could inhibit invasion and metastasis, and was downregulated in non-small lung cancer by targeting Snai1 which was a known transcriptional repressor of E-cadherin and modulator of epithelial-to-mesenchymal transition (EMT) (Kumarswamy et al., 2012). Moreover, in a systematic approach looking for metastatic drivers in colorectal cancer, three miRNAs, miR-218, miR-135b, and miR-210, were identified as key molecules of an EMT-regulating network acting through a number of novel targets including SIAH1, SETD2, ZEB2 and especially FOXN3, which suppressed the transcription of N-cadherin. The modulation of N-cadherin impacted on the migration, invasion and metastasis of cancer cells (Mudduluru et al., 2015). Taken together, miRNAs are potent regulators of metastasis controlling migration, invasion, intravasation, EMT, metastatic colonization and even ATP generation in metastasis sites.

miR-122 abates colorectal cancer metastasis

Bioinformatics analysis and subsequent validation of our whole genome sequencing generated data showed that the miR-122 gene locus was deleted in primary tumors and corresponding metastases of most patients. Interestingly, while the expression of miR-122 was suppressed in primary tumors, it was significantly increased in metastatic lesions (Mudduluru et al., 2015). This suggested that the loss of miR-122 was needed to foster metastatic dissemination, but was again needed for colonization.

The altered expression of miR-122 has been observed in hepatocellular carcinoma, viral hepatitis and hepatic fibrosis. Several studies demonstrated the role of miR-122 in

hepatocellular carcinoma by investigating human tissue, plasma and serum samples as well as cell lines (Coulouarn et al., 2009; Koberle et al., 2013; Tsai et al., 2009). A study by Iino et al. revealed that the most abundant miRNA in liver metastasis compared with primary tumors of CRC was miR-122 (Iino et al., 2013). Another study by Carter et al. measured plasma samples of non-metastatic and metastatic colon cancer patients. They found that increased miR-122 levels were associated with a ‘bad’ prognostic subtype in metastatic CRC and also in non-metastatic CRC patients resulting in shorter relapse-free survival (RFS) and overall survival (OS) times (Carter et al., 2016).

Exosomes mediate paracrine activity of miR-122

In our experiments, the expression of miR-122 in metastatic lesions was surprisingly very high despite the deletion of the miR-122 gene locus in the metastatic lesions. This paradoxical finding has never been reported before. Also, no reports had figured out the mechanism of miR-122 expression aberrations in colorectal cancer cells. Since the liver is rich in miR-122, we postulated that a paracrine mechanism could be involved in the transfer of miR-122 to the metastasized colorectal cancer cells. Consistently, our results showed that miR-122 expression was low/absent in all the colorectal cancer cell lines screened, whereas it was very highly expressed only in Huh7 cells, a hepatocellular carcinoma cell line.

Extracellular factors can affect miRNA expression of normal and cancer cells and miRNAs can also be directly transported to the extracellular space and to other cells through exosomes (Gibbins, Ciaudo, Erhardt, & Voinnet, 2009). A substantial amount of research has been done in order to understand exosome-mediated cell–cell communication mechanisms. Various facets of material transport across biological membranes and the role of exosomes in disease development have been revealed. In fact, every type of protein, RNA (including miRNAs), (Vinciguerra & Stutz, 2004), breakdown product of signaling pathways and even viruses can be transported through exosomes (Fevrier, Vilette, Laude, & Raposo, 2005).

Exosome-mediated miRNA transfer has been established as a mechanism of regulating intercellular communications (Valadi et al., 2007). Koga and colleagues demonstrated that exosomes or cellular membrane could prevent RNase from degrading miRNAs inside the exosome or cells, even in a dreadful condition, as in feces (Koga et al., 2011). Their study proved that miRNA integrity and function were maintained in an exosomal cushion when

transferred to distant sites. Since then, many groups revealed the potential use of exosomal miRNAs for diagnostic and prognostic purposes in lung (Zhou et al., 2017), prostate (Russo et al., 2012), ovarian (Li et al., 2017), breast (Yuan et al., 2012), colon (Hosseini et al., 2017), leukemia (Prieto et al., 2017), and other types of cancer. Moreover, exosome-secreted miRNAs have been shown to induce a number of biological functions including modulation of immune response and modulation of proteases, adhesion molecules, chemokine ligands, cell cycle and angiogenesis-promoting genes, and genes engaged in oxidative stress response. For instance, it has been showed that exosome-secreted oncogenic miRNAs enhance the invasive potential of breast cancer cell lines (Yang et al., 2011).

In this project, we found that miR-122 was secreted in the conditioned media and exosomes of Huh7 cells, which means that miR-122, could be transferred extracellularly through exosomes. Consistently, several reports also demonstrated that miR-122 could be detected in patients' serum exosomes (Selmaj et al., 2017). Furthermore, we observed an increase of miR-122 expression in RKO cells from the third day of co-culture with Huh7 cells. This expression was still significantly enhanced on the fourth and fifth days. On the other hand, miR-122 expression was significantly upregulated in RKO and DLD1 cells when we directly added the exosomes extracted from conditioned media of Huh7 cells into their normal medium respectively. These two approaches both demonstrated that colorectal cancer cells could take up miR-122 secreted from Huh7 cells. This explains our previous paradoxical finding and elucidates where the overexpression miR-122 came from. To date, there are no reports about an exosomal interaction involving the delivery of miR-122 to colorectal cancer cells. However, the transfer of miR-122 via exosomes was documented to occur between human hepatoma cells, Huh7 and HepG2, grown in co-culture. In a reciprocal process, HepG2 secreted Insulin-like Growth Factor 1 (IGF1) that decreased miR-122 expression in Huh7 cells while exosomal miR-122, expressed and released by Huh7, could reduce growth and proliferation of recipient HepG2 cells (Basu & Bhattacharyya, 2014). A study by Lou et al. also showed that adipose tissue-derived mesenchymal stem cells (AMSCs)-derived exosomes could deliver miR-122 into hepatocellular carcinoma cells *in vitro* and altered miR-122-target gene expression, thereby rendering cancer cells sensitive to chemotherapeutic agents through an alteration of miR-122-target gene expression in hepatocellular carcinoma cells (Lou et al., 2015). In addition, miR-122 was highly secreted by breast cancer cells into extracellular vesicles, including exosomes, and mechanistically suppressed glucose uptake by niche cells *in vitro* and *in vivo* by downregulating the glycolytic enzyme pyruvate kinase (PKM) (Fong et

al., 2015). Interestingly, the studies of Basu & Bhattacharyya and Lou et al., and other studies about hepatocellular carcinoma, showed that miR-122 secreted from hepatoma cells or hepatocellular carcinoma cells, could repress target mRNAs, thereby reducing growth and proliferation of recipient cells. This means that in the liver, miR-122 plays a role as a tumor suppressor in most cases. In the study by Fong et al., the authors found that although miR-122 reduced primary tumour growth, it also facilitated metastasis by increasing nutrient availability in the pre-metastatic niche, and *in vivo* inhibition of miR-122 restored glucose uptake in distant organs and decreased the incidence of metastasis. In this case, miR-122 could promote metastasis.

Molecular mediators of miR-122 induced metastasis suppression

We identified and validated two novel target genes of miR-122, RIMS1 and RABL6. A significant reduction was observed in luciferase reporter activity of both 3' UTRs when we treated cell lines with the corresponding miRNA-mimics. This was paralleled by a reduction in mRNA expression of RIMS1 and RABL6 and in protein expression of RABL6. RIMS1 is a member of the RAS gene superfamily and regulates synaptic vesicle exocytosis. It also regulates voltage-gated calcium channels during neurotransmitter and insulin release. This protein exists mainly in the brain and is rarely expressed in the colon or liver (Fagerberg et al., 2014). This is consistent with our Western blot results for RIMS1 in which we could hardly detect this protein.

RABL6, also known as C9orf86 (chromosome 9 open reading frame 86), or RBEL1 (Rab-like protein 1), is a novel subfamily within the Ras superfamily. Montalbano et al. found that RABL6 was overexpressed in about 67% of primary breast cancer (Montalbano, Jin, Sheikh, & Huang, 2007), and a knockdown of it RBEL1 resulted in cell growth suppression, which is associated with morphological and biochemical features of apoptosis as well as the inhibition of extracellular signal-regulated kinase phosphorylation. There are four isoforms of RABL6 (A, B, C, and D), whereby the larger A and B isoforms are mainly GTP-bound, the smaller C and D variants bind to both GTP and GDP (Montalbano, Lui, Sheikh, & Huang, 2009). Furthermore, RABL6A was defined to function as a p53 negative regulator that facilitates MDM2-dependent p53 ubiquitylation and degradation (Lui et al., 2013). Some other groups also found that RABL6A was an oncogene such as it could promote G1 progression in neuroendocrine tumors (NET) by inactivating Rb1, an established suppressor of cancer cell

proliferation and development (Hagen et al., 2014). There are no reports up to now implicating RABL6 in colorectal cancer. Most of the published reports revolve around breast cancer. Consistent with these above published results, in our study, we found that P21 protein was upregulated in RABL6 knockdown CRC cells or CRC cells treated by miR-122. This suggested that miR-122 induced suppression of RABL6 caused a upregulation of P21, although the mechanism by which RABL6 controls P21 is still unknown. P21 is a p53 transcriptional target and cell cycle inhibitor that blocks cyclin-dependent kinase (Cdk)-mediated phosphorylation of the retinoblastoma protein (Rb1) (Sherr & McCormick, 2002).

Furthermore, our data also demonstrated that forced overexpression of miR-122 significantly suppressed cell proliferation and colony formation in at least 2 different CRC cell lines. No significant difference in cell invasion/migration was however observed, possibly due to the function of the main target gene, RABL6.

Taken together, our findings suggest that miR-122 is an important anti-oncogene in colorectal cancer and regulates tumor growth by multiple mechanisms including the silencing of RABL6 as well as enhancing P21 activation. This activity in the context of liver metastasis implicates miR-122 as a potential line of defence against the establishment of liver metastasis and also supports a potential use of miR-122 in the therapy of advanced CRC with liver metastasis.

6 CONCLUSION

Metastasis is the leading cause of colorectal cancer (CRC) deaths and the liver is the most common metastasis site. Nearly 50% - 60% CRC patients are diagnosed with synchronous metastases, 80% of which have liver metastases. Metastasis itself is not a single process but rather, a constellation of multiple events that culminate with the colonization of distant sites by the primary tumor.

As preliminary work for the project of this thesis, the whole genomes of 12 patients with advanced colorectal cancer were sequenced with the Illumina next generation sequencing platform in the Allgayer department. Bioinformatics analysis and subsequent validation showed that the miR-122 gene locus was deleted in primary tumors and corresponding metastases of most patients. Interestingly, while the expression of miR-122 was suppressed in primary tumors, it was significantly increased in metastatic lesions. miR-122 itself is highly abundant and specific to the liver and this microRNA plays a critical role in liver homeostasis by regulating the expression of a large number of target mRNAs and also by suppressing non-hepatic genes.

We found that miR-122 was secreted in the conditioned media and exosomes of Huh7 liver cancer cells, which meant that miR-122, could be potentially transferred extracellularly through exosomes. Furthermore, in co-culture experiments, we observed an increase of miR-122 expression in RKO cells from the third day of co-culture with Huh7 cells. This expression was still significantly enhanced on the fourth and fifth days. On the other hand, miR-122 expression was significantly upregulated in RKO and DLD1 cells when we directly added the exosomes extracted from conditioned media of Huh7 cells into their normal medium, respectively. These two approaches both demonstrated that colorectal cancer cells could take up miR-122 secreted from Huh7 cells. This explains our previous paradoxical finding and elucidates where the overexpression of miR-122 in the colon cancer cells came from. To date, there are no reports about an exosomal interaction involving the delivery of miR-122 to colorectal cancer cells in a paracrine fashion.

We identified and validated two novel target genes of miR-122, RIMS1 and RABL6. RIMS1 is a member of the RAS gene superfamily and regulates synaptic vesicle exocytosis. It also regulates voltage-gated calcium channels during neurotransmitter and insulin release. This protein has not been reported yet to be expressed in the colon or liver. RABL6, also known as

C9orf86 (chromosome 9 open reading frame 86), or RBEL1 (Rab-like protein 1), is a novel subfamily within the Ras superfamily. There are no reports implicating RABL6 in colorectal cancer. In our study, we found that P21 protein was upregulated in RABL6 knockdown CRC cells, or CRC cells treated with active miR-122. This suggested that the miR-122 induced suppression of RABL6 caused a upregulation of P21, although the mechanism by which RABL6 controls P21 is still unknown.

Our data also demonstrated that forced overexpression of miR-122 significantly suppressed cell proliferation and colony formation in at least 2 different CRC cell lines. No significant difference in cell invasion/migration was however observed, possibly due to the function of the main target gene, RABL6.

In general, our findings suggest that miR-122 is a tumor suppressor in colorectal cancer, and regulates tumor growth by multiple mechanisms including the silencing of RABL6 as well as enhancing P21 activation. This particular activity in the context of liver metastasis implicates miR-122 as a potential line of defence against the establishment of CRC liver metastasis, and also supports a potential use of miR-122 in the therapy of advanced CRC with liver metastasis.

7 References

- Ambros, V. (2004). The functions of animal microRNAs. *Nature*, 431(7006), 350-355. doi:10.1038/nature02871
- Asangani, I. A., Rasheed, S. A., Nikolova, D. A., Leupold, J. H., Colburn, N. H., Post, S., & Allgayer, H. (2008). MicroRNA-21 (miR-21) post-transcriptionally downregulates tumor suppressor Pdc4 and stimulates invasion, intravasation and metastasis in colorectal cancer. *Oncogene*, 27(15), 2128-2136. doi:10.1038/sj.onc.1210856
- Baffa, R., Fassan, M., Volinia, S., O'Hara, B., Liu, C. G., Palazzo, J. P., . . . Rosenberg, A. (2009). MicroRNA expression profiling of human metastatic cancers identifies cancer gene targets. *J Pathol*, 219(2), 214-221. doi:10.1002/path.2586
- Basu, S., & Bhattacharyya, S. N. (2014). Insulin-like growth factor-1 prevents miR-122 production in neighbouring cells to curtail its intercellular transfer to ensure proliferation of human hepatoma cells. *Nucleic Acids Res*, 42(11), 7170-7185. doi:10.1093/nar/gku346
- Bentwich, I., Avniel, A., Karov, Y., Aharonov, R., Gilad, S., Barad, O., . . . Bentwich, Z. (2005). Identification of hundreds of conserved and nonconserved human microRNAs. *Nat Genet*, 37(7), 766-770. doi:10.1038/ng1590
- Bitarte, N., Bandres, E., Boni, V., Zarate, R., Rodriguez, J., Gonzalez-Huarriz, M., . . . Garcia-Foncillas, J. (2011). MicroRNA-451 is involved in the self-renewal, tumorigenicity, and chemoresistance of colorectal cancer stem cells. *Stem Cells*, 29(11), 1661-1671. doi:10.1002/stem.741
- Blasi, F., & Carmeliet, P. (2002). uPAR: a versatile signalling orchestrator. *Nat Rev Mol Cell Biol*, 3(12), 932-943. doi:10.1038/nrm977
- Bommer, G. T., Gerin, I., Feng, Y., Kaczorowski, A. J., Kuick, R., Love, R. E., . . . Fearon, E. R. (2007). p53-mediated activation of miRNA34 candidate tumor-suppressor genes. *Curr Biol*, 17(15), 1298-1307. doi:10.1016/j.cub.2007.06.068
- Bosset, J. F., Calais, G., Mineur, L., Maingon, P., Stojanovic-Rundic, S., Bensadoun, R. J., . . . Group, E. R. O. (2014). Fluorouracil-based adjuvant chemotherapy after preoperative chemoradiotherapy in rectal cancer: long-term results of the EORTC 22921 randomised study. *Lancet Oncol*, 15(2), 184-190. doi:10.1016/S1470-2045(13)70599-0
- Burchard, J., Zhang, C., Liu, A. M., Poon, R. T., Lee, N. P., Wong, K. F., . . . Luk, J. M. (2010). microRNA-122 as a regulator of mitochondrial metabolic gene network in hepatocellular carcinoma. *Mol Syst Biol*, 6, 402. doi:10.1038/msb.2010.58
- Cappuzzo, F., Sacconi, A., Landi, L., Ludovini, V., Biagioni, F., D'Incecco, A., . . . Blandino, G. (2014). MicroRNA signature in metastatic colorectal cancer patients treated with anti-EGFR monoclonal antibodies. *Clin Colorectal Cancer*, 13(1), 37-45 e34. doi:10.1016/j.clcc.2013.11.006
- Carmeliet, P., & Jain, R. K. (2011). Principles and mechanisms of vessel normalization for cancer and other angiogenic diseases. *Nat Rev Drug Discov*, 10(6), 417-427. doi:10.1038/nrd3455
- Carter, J. V., Roberts, H. L., Pan, J., Rice, J. D., Burton, J. F., Galbraith, N. J., . . . Galandiuk, S. (2016). A Highly Predictive Model for Diagnosis of Colorectal Neoplasms Using Plasma MicroRNA: Improving Specificity and Sensitivity. *Ann Surg*, 264(4), 575-584. doi:10.1097/SLA.0000000000001873

- Ceppi, P., Mudduluru, G., Kumarswamy, R., Rapa, I., Scagliotti, G. V., Papotti, M., & Allgayer, H. (2010). Loss of miR-200c expression induces an aggressive, invasive, and chemoresistant phenotype in non-small cell lung cancer. *Mol Cancer Res*, 8(9), 1207-1216. doi:10.1158/1541-7786.MCR-10-0052
- Chang, J., Nicolas, E., Marks, D., Sander, C., Lerro, A., Buendia, M. A., . . . Taylor, J. M. (2004). miR-122, a mammalian liver-specific microRNA, is processed from hcr mRNA and may downregulate the high affinity cationic amino acid transporter CAT-1. *RNA Biol*, 1(2), 106-113.
- Chang, T. C., Wentzel, E. A., Kent, O. A., Ramachandran, K., Mullendore, M., Lee, K. H., . . . Mendell, J. T. (2007). Transactivation of miR-34a by p53 broadly influences gene expression and promotes apoptosis. *Mol Cell*, 26(5), 745-752. doi:10.1016/j.molcel.2007.05.010
- Coghlin, C., & Murray, G. I. (2010). Current and emerging concepts in tumour metastasis. *J Pathol*, 222(1), 1-15. doi:10.1002/path.2727
- Conrad, T., Marsico, A., Gehre, M., & Orom, U. A. (2014). Microprocessor activity controls differential miRNA biogenesis In Vivo. *Cell Rep*, 9(2), 542-554. doi:10.1016/j.celrep.2014.09.007
- Coulouarn, C., Factor, V. M., Andersen, J. B., Durkin, M. E., & Thorgeirsson, S. S. (2009). Loss of miR-122 expression in liver cancer correlates with suppression of the hepatic phenotype and gain of metastatic properties. *Oncogene*, 28(40), 3526-3536. doi:10.1038/onc.2009.211
- Dvorak, H. F. (1986). Tumors: wounds that do not heal. Similarities between tumor stroma generation and wound healing. *N Engl J Med*, 315(26), 1650-1659. doi:10.1056/NEJM198612253152606
- El-Daly, S. M., Abba, M. L., Patil, N., & Allgayer, H. (2016). miRs-134 and -370 function as tumor suppressors in colorectal cancer by independently suppressing EGFR and PI3K signalling. *Sci Rep*, 6, 24720. doi:10.1038/srep24720
- Esau, C., Davis, S., Murray, S. F., Yu, X. X., Pandey, S. K., Pear, M., . . . Monia, B. P. (2006). miR-122 regulation of lipid metabolism revealed by in vivo antisense targeting. *Cell Metab*, 3(2), 87-98. doi:10.1016/j.cmet.2006.01.005
- Eulalio, A., Huntzinger, E., Nishihara, T., Rehwinkel, J., Fauser, M., & Izaurralde, E. (2009). Deadenylation is a widespread effect of miRNA regulation. *RNA*, 15(1), 21-32. doi:10.1261/rna.1399509
- Fagerberg, L., Hallstrom, B. M., Oksvold, P., Kampf, C., Djureinovic, D., Odeberg, J., . . . Uhlen, M. (2014). Analysis of the human tissue-specific expression by genome-wide integration of transcriptomics and antibody-based proteomics. *Mol Cell Proteomics*, 13(2), 397-406. doi:10.1074/mcp.M113.035600
- Fevrier, B., Vilette, D., Laude, H., & Raposo, G. (2005). Exosomes: a bubble ride for prions? *Traffic*, 6(1), 10-17. doi:10.1111/j.1600-0854.2004.00247.x
- Fish, J. E., Santoro, M. M., Morton, S. U., Yu, S., Yeh, R. F., Wythe, J. D., . . . Srivastava, D. (2008). miR-126 regulates angiogenic signaling and vascular integrity. *Dev Cell*, 15(2), 272-284. doi:10.1016/j.devcel.2008.07.008
- Fong, M. Y., Zhou, W., Liu, L., Alontaga, A. Y., Chandra, M., Ashby, J., . . . Wang, S. E. (2015). Breast-cancer-secreted miR-122 reprograms glucose metabolism in premetastatic niche to promote metastasis. *Nat Cell Biol*, 17(2), 183-194. doi:10.1038/ncb3094
- Fu, H., Tie, Y., Xu, C., Zhang, Z., Zhu, J., Shi, Y., . . . Zheng, X. (2005). Identification of human fetal liver miRNAs by a novel method. *FEBS Lett*, 579(17), 3849-3854. doi:10.1016/j.febslet.2005.05.064

- Gaedcke, J., Grade, M., Camps, J., Sokilde, R., Kaczkowski, B., Schetter, A. J., . . . Litman, T. (2012). The rectal cancer microRNAome--microRNA expression in rectal cancer and matched normal mucosa. *Clin Cancer Res*, 18(18), 4919-4930. doi:10.1158/1078-0432.CCR-12-0016
- Geho, D. H., Bandle, R. W., Clair, T., & Liotta, L. A. (2005). Physiological mechanisms of tumor-cell invasion and migration. *Physiology (Bethesda)*, 20, 194-200. doi:10.1152/physiol.00009.2005
- Giampieri, R., Scartozzi, M., Del Prete, M., Maccaroni, E., Bittoni, A., Faloppi, L., . . . Cascinu, S. (2013). Molecular biomarkers of resistance to anti-EGFR treatment in metastatic colorectal cancer, from classical to innovation. *Crit Rev Oncol Hematol*, 88(2), 272-283. doi:10.1016/j.critrevonc.2013.05.008
- Gibbins, D. J., Ciaudo, C., Erhardt, M., & Voinnet, O. (2009). Multivesicular bodies associate with components of miRNA effector complexes and modulate miRNA activity. *Nat Cell Biol*, 11(9), 1143-1149. doi:10.1038/ncb1929
- Hagen, J., Muniz, V. P., Falls, K. C., Reed, S. M., Taghiyev, A. F., Quelle, F. W., . . . Quelle, D. E. (2014). RABL6A promotes G1-S phase progression and pancreatic neuroendocrine tumor cell proliferation in an Rb1-dependent manner. *Cancer Res*, 74(22), 6661-6670. doi:10.1158/0008-5472.CAN-13-3742
- He, L., Thomson, J. M., Hemann, M. T., Hernando-Monge, E., Mu, D., Goodson, S., . . . Hammond, S. M. (2005). A microRNA polycistron as a potential human oncogene. *Nature*, 435(7043), 828-833. doi:10.1038/nature03552
- Hosseini, M., Khatamianfar, S., Hassanian, S. M., Nedaeinia, R., Shafiee, M., Maftouh, M., . . . Avan, A. (2017). Exosome-Encapsulated microRNAs as Potential Circulating Biomarkers in Colon Cancer. *Curr Pharm Des*, 23(11), 1705-1709. doi:10.2174/1381612822666161201144634
- Hsu, S. H., Delgado, E. R., Otero, P. A., Teng, K. Y., Kutay, H., Meehan, K. M., . . . Duncan, A. W. (2016). MicroRNA-122 regulates polyploidization in the murine liver. *Hepatology*, 64(2), 599-615. doi:10.1002/hep.28573
- Hur, K., Toiyama, Y., Schetter, A. J., Okugawa, Y., Harris, C. C., Boland, C. R., & Goel, A. (2015). Identification of a metastasis-specific MicroRNA signature in human colorectal cancer. *J Natl Cancer Inst*, 107(3). doi:10.1093/jnci/dju492
- Iino, I., Kikuchi, H., Miyazaki, S., Hiramatsu, Y., Ohta, M., Kamiya, K., . . . Konno, H. (2013). Effect of miR-122 and its target gene cationic amino acid transporter 1 on colorectal liver metastasis. *Cancer Sci*, 104(5), 624-630. doi:10.1111/cas.12122
- Jemal, A., Bray, F., Center, M. M., Ferlay, J., Ward, E., & Forman, D. (2011). Global cancer statistics. *CA Cancer J Clin*, 61(2), 69-90. doi:10.3322/caac.20107
- Jiang, W. G., Puntis, M. C., & Hallett, M. B. (1994). Molecular and cellular basis of cancer invasion and metastasis: implications for treatment. *Br J Surg*, 81(11), 1576-1590.
- Jopling, C. L., Yi, M., Lancaster, A. M., Lemon, S. M., & Sarnow, P. (2005). Modulation of hepatitis C virus RNA abundance by a liver-specific MicroRNA. *Science*, 309(5740), 1577-1581. doi:10.1126/science.1113329
- Kessenbrock, K., Plaks, V., & Werb, Z. (2010). Matrix metalloproteinases: regulators of the tumor microenvironment. *Cell*, 141(1), 52-67. doi:10.1016/j.cell.2010.03.015
- Klein, C. A. (2003). The systemic progression of human cancer: a focus on the individual disseminated cancer cell--the unit of selection. *Adv Cancer Res*, 89, 35-67.

- Klein, C. A. (2009). Parallel progression of primary tumours and metastases. *Nat Rev Cancer*, 9(4), 302-312. doi:10.1038/nrc2627
- Koberle, V., Kronenberger, B., Pleli, T., Trojan, J., Imelmann, E., Peveling-Oberhag, J., . . . Waidmann, O. (2013). Serum microRNA-1 and microRNA-122 are prognostic markers in patients with hepatocellular carcinoma. *Eur J Cancer*, 49(16), 3442-3449. doi:10.1016/j.ejca.2013.06.002
- Koga, Y., Yasunaga, M., Moriya, Y., Akasu, T., Fujita, S., Yamamoto, S., & Matsumura, Y. (2011). Exosome can prevent RNase from degrading microRNA in feces. *J Gastrointest Oncol*, 2(4), 215-222. doi:10.3978/j.issn.2078-6891.2011.015
- Kruger, A. (2015). Premetastatic niche formation in the liver: emerging mechanisms and mouse models. *J Mol Med (Berl)*, 93(11), 1193-1201. doi:10.1007/s00109-015-1342-7
- Krutzfeldt, J., Rajewsky, N., Braich, R., Rajeev, K. G., Tuschl, T., Manoharan, M., & Stoffel, M. (2005). Silencing of microRNAs in vivo with 'antagomirs'. *Nature*, 438(7068), 685-689. doi:10.1038/nature04303
- Kumarswamy, R., Mudduluru, G., Ceppi, P., Muppala, S., Kozlowski, M., Niklinski, J., . . . Allgayer, H. (2012). MicroRNA-30a inhibits epithelial-to-mesenchymal transition by targeting Snai1 and is downregulated in non-small cell lung cancer. *Int J Cancer*, 130(9), 2044-2053. doi:10.1002/ijc.26218
- Landgraf, P., Rusu, M., Sheridan, R., Sewer, A., Iovino, N., Aravin, A., . . . Tuschl, T. (2007). A mammalian microRNA expression atlas based on small RNA library sequencing. *Cell*, 129(7), 1401-1414. doi:10.1016/j.cell.2007.04.040
- Laudadio, I., Manfredi, I., Achouri, Y., Schmidt, D., Wilson, M. D., Cordi, S., . . . Lemaigre, F. P. (2012). A feedback loop between the liver-enriched transcription factor network and miR-122 controls hepatocyte differentiation. *Gastroenterology*, 142(1), 119-129. doi:10.1053/j.gastro.2011.09.001
- Laudato, S., Patil, N., Abba, M. L., Leupold, J. H., Benner, A., Gaiser, T., . . . Allgayer, H. (2017). P53-induced miR-30e-5p inhibits colorectal cancer invasion and metastasis by targeting ITGA6 and ITGB1. *Int J Cancer*, 141(9), 1879-1890. doi:10.1002/ijc.30854
- Lee, Y., Kim, M., Han, J., Yeom, K. H., Lee, S., Baek, S. H., & Kim, V. N. (2004). MicroRNA genes are transcribed by RNA polymerase II. *EMBO J*, 23(20), 4051-4060. doi:10.1038/sj.emboj.7600385
- Lewis, B. P., Burge, C. B., & Bartel, D. P. (2005). Conserved seed pairing, often flanked by adenosines, indicates that thousands of human genes are microRNA targets. *Cell*, 120(1), 15-20. doi:10.1016/j.cell.2004.12.035
- Li, Y., Yang, Y., Xiong, A., Wu, X., Xie, J., Han, S., & Zhao, S. (2017). Comparative Gene Expression Analysis of Lymphocytes Treated with Exosomes Derived from Ovarian Cancer and Ovarian Cysts. *Front Immunol*, 8, 607. doi:10.3389/fimmu.2017.00607
- Lin, C. J., Gong, H. Y., Tseng, H. C., Wang, W. L., & Wu, J. L. (2008). miR-122 targets an anti-apoptotic gene, Bcl-w, in human hepatocellular carcinoma cell lines. *Biochem Biophys Res Commun*, 375(3), 315-320. doi:10.1016/j.bbrc.2008.07.154
- Ling, H., Pickard, K., Ivan, C., Isella, C., Ikuo, M., Mitter, R., . . . Nicoloso, M. S. (2016). The clinical and biological significance of MIR-224 expression in colorectal cancer metastasis. *Gut*, 65(6), 977-989. doi:10.1136/gutjnl-2015-309372

- Loffler, D., Brocke-Heidrich, K., Pfeifer, G., Stocsits, C., Hackermuller, J., Kretzschmar, A. K., . . . Horn, F. (2007). Interleukin-6 dependent survival of multiple myeloma cells involves the Stat3-mediated induction of microRNA-21 through a highly conserved enhancer. *Blood*, 110(4), 1330-1333. doi:10.1182/blood-2007-03-081133
- Loo, J. M., Scherl, A., Nguyen, A., Man, F. Y., Weinberg, E., Zeng, Z., . . . Tavazoie, S. F. (2015). Extracellular metabolic energetics can promote cancer progression. *Cell*, 160(3), 393-406. doi:10.1016/j.cell.2014.12.018
- Lou, G., Song, X., Yang, F., Wu, S., Wang, J., Chen, Z., & Liu, Y. (2015). Exosomes derived from miR-122-modified adipose tissue-derived MSCs increase chemosensitivity of hepatocellular carcinoma. *J Hematol Oncol*, 8, 122. doi:10.1186/s13045-015-0220-7
- Lu, J., Getz, G., Miska, E. A., Alvarez-Saavedra, E., Lamb, J., Peck, D., . . . Golub, T. R. (2005). MicroRNA expression profiles classify human cancers. *Nature*, 435(7043), 834-838. doi:10.1038/nature03702
- Lui, K., An, J., Montalbano, J., Shi, J., Corcoran, C., He, Q., . . . Huang, Y. (2013). Negative regulation of p53 by Ras superfamily protein RBEL1A. *J Cell Sci*, 126(Pt 11), 2436-2445. doi:10.1242/jcs.118117
- Lund, E., & Dahlberg, J. E. (2006). Substrate selectivity of exportin 5 and Dicer in the biogenesis of microRNAs. *Cold Spring Harb Symp Quant Biol*, 71, 59-66. doi:10.1101/sqb.2006.71.050
- Massague, J., & Obenauf, A. C. (2016). Metastatic colonization by circulating tumour cells. *Nature*, 529(7586), 298-306. doi:10.1038/nature17038
- Matsubara, H., Takeuchi, T., Nishikawa, E., Yanagisawa, K., Hayashita, Y., Ebi, H., . . . Takahashi, T. (2007). Apoptosis induction by antisense oligonucleotides against miR-17-5p and miR-20a in lung cancers overexpressing miR-17-92. *Oncogene*, 26(41), 6099-6105. doi:10.1038/sj.onc.1210425
- McAllister, S. S., & Weinberg, R. A. (2014). The tumour-induced systemic environment as a critical regulator of cancer progression and metastasis. *Nat Cell Biol*, 16(8), 717-727. doi:10.1038/ncb3015
- McGowan, P. M., Kirstein, J. M., & Chambers, A. F. (2009). Micrometastatic disease and metastatic outgrowth: clinical issues and experimental approaches. *Future Oncol*, 5(7), 1083-1098. doi:10.2217/fon.09.73
- Meng, F., Henson, R., Wehbe-Janek, H., Ghoshal, K., Jacob, S. T., & Patel, T. (2007). MicroRNA-21 regulates expression of the PTEN tumor suppressor gene in human hepatocellular cancer. *Gastroenterology*, 133(2), 647-658. doi:10.1053/j.gastro.2007.05.022
- Minna, J. D., Kurie, J. M., & Jacks, T. (2003). A big step in the study of small cell lung cancer. *Cancer Cell*, 4(3), 163-166.
- Montalbano, J., Jin, W., Sheikh, M. S., & Huang, Y. (2007). RBEL1 is a novel gene that encodes a nucleocytoplasmic Ras superfamily GTP-binding protein and is overexpressed in breast cancer. *J Biol Chem*, 282(52), 37640-37649. doi:10.1074/jbc.M704760200
- Montalbano, J., Lui, K., Sheikh, M. S., & Huang, Y. (2009). Identification and characterization of RBEL1 subfamily of GTPases in the Ras superfamily involved in cell growth regulation. *J Biol Chem*, 284(27), 18129-18142. doi:10.1074/jbc.M109.009597
- Mudduluru, G., Abba, M., Batliner, J., Patil, N., Scharp, M., Lunavat, T. R., . . . Allgayer, H. (2015). A Systematic Approach to Defining the microRNA

- Landscape in Metastasis. *Cancer Res*, 75(15), 3010-3019. doi:10.1158/0008-5472.CAN-15-0997
- Mudduluru, G., Ceppi, P., Kumarswamy, R., Scagliotti, G. V., Papotti, M., & Allgayer, H. (2011). Regulation of Axl receptor tyrosine kinase expression by miR-34a and miR-199a/b in solid cancer. *Oncogene*, 30(25), 2888-2899. doi:10.1038/onc.2011.13
- Muppala, S., Mudduluru, G., Leupold, J. H., Buergy, D., Sleeman, J. P., & Allgayer, H. (2013). CD24 induces expression of the oncomir miR-21 via Src, and CD24 and Src are both post-transcriptionally downregulated by the tumor suppressor miR-34a. *PLoS One*, 8(3), e59563. doi:10.1371/journal.pone.0059563
- Nguyen, D. X., Bos, P. D., & Massague, J. (2009). Metastasis: from dissemination to organ-specific colonization. *Nat Rev Cancer*, 9(4), 274-284. doi:10.1038/nrc2622
- Peinado, H., Lavotshkin, S., & Lyden, D. (2011). The secreted factors responsible for pre-metastatic niche formation: old sayings and new thoughts. *Semin Cancer Biol*, 21(2), 139-146. doi:10.1016/j.semcancer.2011.01.002
- Poste, G., & Fidler, I. J. (1980). The pathogenesis of cancer metastasis. *Nature*, 283(5743), 139-146.
- Prieto, D., Sotelo, N., Seija, N., Sernbo, S., Abreu, C., Duran, R., . . . Oppezzo, P. (2017). S100-A9 protein in exosomes from chronic lymphocytic leukemia cells promotes NF-kappaB activity during disease progression. *Blood*, 130(6), 777-788. doi:10.1182/blood-2017-02-769851
- Rinaldi, A., Poretti, G., Kwee, I., Zucca, E., Catapano, C. V., Tibiletti, M. G., & Bertoni, F. (2007). Concomitant MYC and microRNA cluster miR-17-92 (C13orf25) amplification in human mantle cell lymphoma. *Leuk Lymphoma*, 48(2), 410-412. doi:10.1080/10428190601059738
- Russo, L. M., Bate, K., Motamedinia, P., Salazar, G., Scott, A., Lipsky, M., . . . McKiernan, J. M. (2012). Urinary exosomes as a stable source of mRNA for prostate cancer analysis. *J Clin Oncol*, 30(5_suppl), 174. doi:10.1200/jco.2012.30.5_suppl.174
- Selmaj, I., Cichalewska, M., Namiecinska, M., Galazka, G., Horzelski, W., Selmaj, K. W., & Mycko, M. P. (2017). Global exosome transcriptome profiling reveals biomarkers for multiple sclerosis. *Ann Neurol*, 81(5), 703-717. doi:10.1002/ana.24931
- Sherr, C. J., & McCormick, F. (2002). The RB and p53 pathways in cancer. *Cancer Cell*, 2(2), 103-112.
- Siegel, R. L., Miller, K. D., Fedewa, S. A., Ahnen, D. J., Meester, R. G., Barzi, A., & Jemal, A. (2017). Colorectal cancer statistics, 2017. *CA Cancer J Clin*. doi:10.3322/caac.21395
- Sosa, M. S., Bragado, P., & Aguirre-Ghiso, J. A. (2014). Mechanisms of disseminated cancer cell dormancy: an awakening field. *Nat Rev Cancer*, 14(9), 611-622. doi:10.1038/nrc3793
- Stangl, R., Altendorf-Hofmann, A., Charnley, R. M., & Scheele, J. (1994). Factors influencing the natural history of colorectal liver metastases. *Lancet*, 343(8910), 1405-1410.
- Steeg, P. S. (2006). Tumor metastasis: mechanistic insights and clinical challenges. *Nat Med*, 12(8), 895-904. doi:10.1038/nm1469
- Strauss, D. C., & Thomas, J. M. (2010). Transmission of donor melanoma by organ transplantation. *Lancet Oncol*, 11(8), 790-796. doi:10.1016/S1470-2045(10)70024-3

- Suto, T., Yokobori, T., Yajima, R., Morita, H., Fujii, T., Yamaguchi, S., . . . Kuwano, H. (2015). MicroRNA-7 expression in colorectal cancer is associated with poor prognosis and regulates cetuximab sensitivity via EGFR regulation. *Carcinogenesis*, 36(3), 338-345. doi:10.1093/carcin/bgu242
- Talmadge, J. E., & Fidler, I. J. (2010). AACR centennial series: the biology of cancer metastasis: historical perspective. *Cancer Res*, 70(14), 5649-5669. doi:10.1158/0008-5472.CAN-10-1040
- Tang, H., Ji, F., Sun, J., Xie, Y., Xu, Y., & Yue, H. (2016). RBEL1 is required for osteosarcoma cell proliferation via inhibiting retinoblastoma 1. *Mol Med Rep*, 13(2), 1275-1280. doi:10.3892/mmr.2015.4670
- Torre, L. A., Bray, F., Siegel, R. L., Ferlay, J., Lortet-Tieulent, J., & Jemal, A. (2015). Global cancer statistics, 2012. *CA Cancer J Clin*, 65(2), 87-108. doi:10.3322/caac.21262
- Tsai, W. C., Hsu, P. W., Lai, T. C., Chau, G. Y., Lin, C. W., Chen, C. M., . . . Tsou, A. P. (2009). MicroRNA-122, a tumor suppressor microRNA that regulates intrahepatic metastasis of hepatocellular carcinoma. *Hepatology*, 49(5), 1571-1582. doi:10.1002/hep.22806
- Turchinovich, A., Weiz, L., & Burwinkel, B. (2012). Extracellular miRNAs: the mystery of their origin and function. *Trends Biochem Sci*, 37(11), 460-465. doi:10.1016/j.tibs.2012.08.003
- Valadi, H., Ekstrom, K., Bossios, A., Sjostrand, M., Lee, J. J., & Lotvall, J. O. (2007). Exosome-mediated transfer of mRNAs and microRNAs is a novel mechanism of genetic exchange between cells. *Nat Cell Biol*, 9(6), 654-659. doi:10.1038/ncb1596
- Valeri, N., Braconi, C., Gasparini, P., Murgia, C., Lampis, A., Paulus-Hock, V., . . . Croce, C. M. (2014). MicroRNA-135b promotes cancer progression by acting as a downstream effector of oncogenic pathways in colon cancer. *Cancer Cell*, 25(4), 469-483. doi:10.1016/j.ccr.2014.03.006
- Van Cutsem, E., Nordlinger, B., Adam, R., Kohne, C. H., Pozzo, C., Poston, G., . . . European Colorectal Metastases Treatment, G. (2006). Towards a pan-European consensus on the treatment of patients with colorectal liver metastases. *Eur J Cancer*, 42(14), 2212-2221. doi:10.1016/j.ejca.2006.04.012
- Van den Eynden, G. G., Majeed, A. W., Illemann, M., Vermeulen, P. B., Bird, N. C., Hoyer-Hansen, G., . . . Brodt, P. (2013). The multifaceted role of the microenvironment in liver metastasis: biology and clinical implications. *Cancer Res*, 73(7), 2031-2043. doi:10.1158/0008-5472.CAN-12-3931
- Vinciguerra, P., & Stutz, F. (2004). mRNA export: an assembly line from genes to nuclear pores. *Curr Opin Cell Biol*, 16(3), 285-292. doi:10.1016/j.ceb.2004.03.013
- Volinia, S., Calin, G. A., Liu, C. G., Ambs, S., Cimmino, A., Petrocca, F., . . . Croce, C. M. (2006). A microRNA expression signature of human solid tumors defines cancer gene targets. *Proc Natl Acad Sci U S A*, 103(7), 2257-2261. doi:10.1073/pnas.0510565103
- Wang, B., Hsu, S. H., Wang, X., Kutay, H., Bid, H. K., Yu, J., . . . Ghoshal, K. (2014). Reciprocal regulation of microRNA-122 and c-Myc in hepatocellular cancer: role of E2F1 and transcription factor dimerization partner 2. *Hepatology*, 59(2), 555-566. doi:10.1002/hep.26712
- Wang, S., Qiu, L., Yan, X., Jin, W., Wang, Y., Chen, L., . . . Meng, S. (2012). Loss of microRNA 122 expression in patients with hepatitis B enhances hepatitis B

- virus replication through cyclin G(1) -modulated P53 activity. *Hepatology*, 55(3), 730-741. doi:10.1002/hep.24809
- Wang, S. C., Lin, X. L., Li, J., Zhang, T. T., Wang, H. Y., Shi, J. W., . . . Xiao, D. (2014). MicroRNA-122 triggers mesenchymal-epithelial transition and suppresses hepatocellular carcinoma cell motility and invasion by targeting RhoA. *PLoS One*, 9(7), e101330. doi:10.1371/journal.pone.0101330
- Wang, X. J., Reyes, J. L., Chua, N. H., & Gaasterland, T. (2004). Prediction and identification of Arabidopsis thaliana microRNAs and their mRNA targets. *Genome Biol*, 5(9), R65. doi:10.1186/gb-2004-5-9-r65
- Williams, A. E. (2008). Functional aspects of animal microRNAs. *Cell Mol Life Sci*, 65(4), 545-562. doi:10.1007/s00018-007-7355-9
- Winter, J., Jung, S., Keller, S., Gregory, R. I., & Diederichs, S. (2009). Many roads to maturity: microRNA biogenesis pathways and their regulation. *Nat Cell Biol*, 11(3), 228-234. doi:10.1038/ncb0309-228
- Wolpin, B. M., & Mayer, R. J. (2008). Systemic treatment of colorectal cancer. *Gastroenterology*, 134(5), 1296-1310. doi:10.1053/j.gastro.2008.02.098
- Xu, H., He, J. H., Xiao, Z. D., Zhang, Q. Q., Chen, Y. Q., Zhou, H., & Qu, L. H. (2010). Liver-enriched transcription factors regulate microRNA-122 that targets CUTL1 during liver development. *Hepatology*, 52(4), 1431-1442. doi:10.1002/hep.23818
- Yang, M., Chen, J., Su, F., Yu, B., Su, F., Lin, L., . . . Song, E. (2011). Microvesicles secreted by macrophages shuttle invasion-potentiating microRNAs into breast cancer cells. *Mol Cancer*, 10, 117. doi:10.1186/1476-4598-10-117
- Yoo, P. S., Lopez-Soler, R. I., Longo, W. E., & Cha, C. H. (2006). Liver resection for metastatic colorectal cancer in the age of neoadjuvant chemotherapy and bevacizumab. *Clin Colorectal Cancer*, 6(3), 202-207. doi:10.3816/CCC.2006.n.036
- Yuan, Y., Valenzuela, M. M., Turay, D., Ferguson, H., Wong, S. F., Perez, M., . . . Wall, N. R. (2012). Early diagnostic value of survivin and its alternative splice variants in breast cancers. *J Clin Oncol*, 30(27_suppl), 35. doi:10.1200/jco.2012.30.27_suppl.35
- Zhou, L., Lv, T., Zhang, Q., Zhu, Q., Zhan, P., Zhu, S., . . . Song, Y. (2017). The biology, function and clinical implications of exosomes in lung cancer. *Cancer Lett*. doi:10.1016/j.canlet.2017.08.003

8 CURRICULUM VITAE

PERSONAL DETAILS

Name: Sha Guan Date of Birth: 14. 03. 1984 Gender: Female

E-mail: guanshachina@hotmail.com Nationality: Chinese

EDUCATION

• 01.2015 – Now Doctor of Medicine

University Heidelberg - Medicine Faculty Mannheim, Germany

• 09. 2002 – 06.2009 Master Degree of Clinical Medicine

Combined Bachelor- Master Degree Program

Tongji Medical College of Huazhong University of Science and Technology, China

WORK EXPERIENCE

• 10. 2012 – 09.2014 Attending Physician

Department of Oncology, Wuhan General Hospital of Guangzhou Military

• 07. 2009 – 10.2012 Resident Physician

Department of Oncology, Wuhan General Hospital of Guangzhou Military

9 ACKNOWLEDGEMENTS

Firstly, I would like to thank my supervisor Prof. Dr. med. Heike Allgayer for providing me the opportunity to study in the Department of Experimental Surgery – Cancer Metastasis, to work on this interesting project, and for giving me a lot of valuable and precious advice on my project and dissertation. She also gave me a lot of help in applying for the China Scholarship Council scholarship and generally, my entire stay in Germany. Without her, I would not have been able to get through a happy and fulfilling three years.

Meanwhile, I would like to thank Dr. Mohammed Abba who patiently taught me how to design a project and perform all experiments, and gave me a lot of help and suggestions. Many thanks to Dr. Joerg Leupold and Dr. Nitin Patil, they kindly taught me basic lab rules and cell culture experiments, and gave me a lot of precious advice. I also owe my thanks to my dearest colleagues, in particular, Dr. Yong Chen, Chan Zhou, Xinmiao Zhang and Sandra Huehl, who never hesitated to offer me their kind help.

I would also like to acknowledge the China Scholarship Council that financed my two-year doctoral study in Germany.

I am also deeply grateful for my lovely friends. Because of them, I had the courage to face and overcome any difficulty.

Last but not least, I would like to thank my husband and parents, they always gave me enormous support and encourage.